

Understanding Ly α emitters

Kim K. Nilsson, Klaus Meisenheimer (Eds.)

Max-Planck-Institut für Astronomie, Königstuhl 17, 69117 Heidelberg, Germany

Abstract

This publication contains the conference summary of the *Understanding Ly α Emitters* conference held at the Max Planck Institute for Astronomy in Heidelberg October 6 - 10, 2008. The scope of the conference was to bring together most of the scientists working in the field of Ly α emitters, whether at low or high redshift, or on observational or theoretical aspects, and to summarise how far the field of study of galaxies with Ly α emission has come. An outlook towards the future of the field was also desired. As part of the conference, two days were dedicated to in total six discussion sessions. The topics were *i)* new methods and selection methods, *ii)* morphology, *iii)* what can the local Universe observations tell us about the high redshift Universe?, *iv)* clustering, *v)* SED fitting and *vi)* Ly α blobs. The chairs of those sessions were asked to summarise the discussions, as presented in these proceedings.

Key words:

conference proceedings, observational cosmology, Ly α emitters, high redshift galaxies

PACS: 98.80.Es

1 Introduction

There are many methods available to find galaxies at high redshift. One method which is getting increasingly popular is that of targeting the Ly α emission of young, star-forming galaxies. This emission can be easily detected both in spectroscopic and imaging surveys (most notably with narrow-band imaging) and has been proven effective from redshift $z = 2 - 7$ to date (e.g. Cowie & Hu 1998; Fynbo et al. 2001; Iye et al. 2006; Venemans et al. 2007; Nilsson et al. 2009). One of the fascinating aspects of Ly α selection is that it targets *star-forming galaxies* mainly. Contributions may also come from so-called cold accretion (Haiman et al. 2000; Fardal et al. 2001; Nilsson et al. 2006; Smith & Jarvis 2007) or AGN activity (Dey et al. 2005; Weidinger et al. 2006), however, cold accretion has so far only been observed in Ly α blobs (see also the contribution of Yamada in these proceedings) and contributions of AGN in normal samples of Ly α emitters (LAEs hereafter) are limited to small percentages ($< 10\%$, Gawiser et al. 2007; Ouchi et al. 2008). Thus, as the method of searching for redshift Ly α emission is not dependent on detecting the

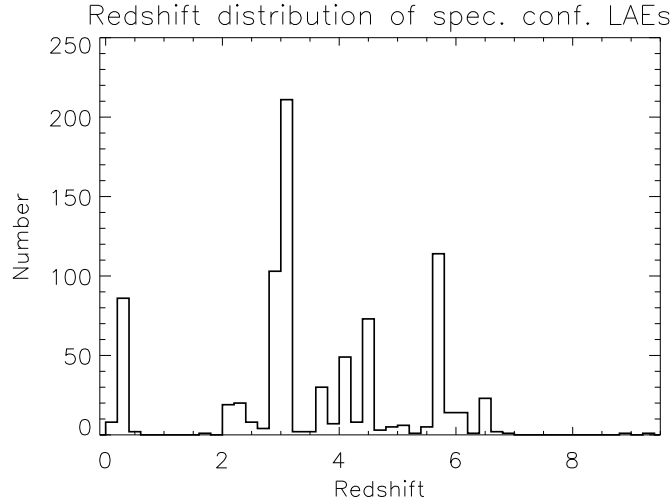


Fig. 1. Redshift distribution of spectroscopically confirmed LAEs. *With a disclaimer that some publications may have been unintentionally overlooked.*

continuum, LAEs are very useful tools to study star-forming galaxies over a large redshift span.

In Fig. 1 the distribution of redshifts of spectroscopically confirmed LAEs to date is shown. It is seen that the largest number of LAEs have been found at $z \sim 3$, presumably due to the high sensitivity of CCDs in the wavelength range around $\sim 5000 \text{ \AA}$ and the availability of narrow-band filters focused on the local [OIII] line. But large samples have also been found at very high redshifts, above $z \sim 5$. It is clear that LAEs are comparably easy to use for observations of the very high redshift Universe, however, to use LAEs as a probe for the high redshift science, we also need to understand the galaxies themselves. This is where lower redshift observations come in. It is only at redshifts below or around three that any real information about the properties and nature of these objects is readily available. For galaxies with redshifts $z \gtrsim 3$ only the restframe UV can be reached in optical and near-IR observations. For these galaxies, it is necessary to rely on Spitzer data to get a handle on the stellar population of the galaxy. For higher redshift objects there is also a large loss in flux due to the increasing luminosity distance and the continuum of the source is in many cases impossible to observe. Thus it is clear that observations at redshifts $z < 3$ are desirable in the understanding of $\text{Ly}\alpha$ emitters. A further advantage with *local* Universe LAEs is that the individual star forming regions within the galaxy can be studied, helping the understanding of the global properties of LAEs.

Studying Fig. 1 shows that there is a lack of objects in this range, due to the difficulty of observing in the ultra-violet. In the local Universe a handful of objects have been observed (Kunth et al. 2003; Östlin et al. 2008), and a sample of 66 LAEs were recently found at $z \sim 0.25$ by Deharveng et al. (2008). At higher redshifts, nine narrow-band surveys have so far been published below $z \sim 3$; Fynbo et al. (1999), Pentericci et al. (2000), Stiavelli et al. (2001), Fynbo et al. (2002, 2003a,b),

Francis et al. (2004), Venemans et al. (2007) and Nilsson et al. (2009). Van Breukelen et al. (2005) furthermore published a sample of Ly α emitters (LAEs) at $z \sim 2.5$ using integral-field spectroscopy. In total, some 300 LAEs have been published with $0 < z < 3$, although the majority of them only in very recent publications. Thus, the understanding of the properties of these low redshift LAEs is just in its beginning.

Theorists are also making progress in predicting the properties of LAEs. Several radiative transfer codes are now being developed for modeling the escape of the Ly α emission, including those of Tasitsiomi (2006), Verhamme et al. (2006) and Laursen et al. (2009). Using these codes, the spectral and surface brightness profiles of LAEs may be interpreted and questions regarding inflow or outflow of material in the galaxies answered. Further clues about the properties of LAEs and other high redshift galaxies come from hydro-dynamical simulations (e.g. Furlanetto et al. 2005; Davé et al. 2006; Nagamine et al. 2008) or semi-analytical modeling (e.g. Le Delliou et al. 2005; 2006; Kobayashi et al. 2007; Mao et al. 2007; Orsi et al. 2008). These models have been able to accurately describe observed quantities such as luminosity functions and clustering results. Some open questions remain though, such as the use and value of Ly α escape fractions and duty cycles.

2 Scientific rationale of conference

The successfully applied technique of narrow-band imaging for Ly α emitters is now more than ten years old, and the sample of known emitters at redshifts between $z = 2 - 7$ is growing rapidly. New and improved technologies allow the high end of the redshift limit to be pushed further, but interest is also growing for the lower redshift ($z = 2 - 3$) observations. As greater samples of Ly α emitters are gathered, there is an increasing desire to try to understand the nature of objects selected in this way. This is most easily achieved working at lower redshifts, where a larger wavelength span can be observed and where the luminosity distance is smaller, thus increasing the signal-to-noise of the detections. New insights can also be gained by comparing the observations with local Universe Ly α emitting galaxies and theoretical models.

In this context the conference was aimed at reviewing what is currently known about the properties, such as ages, SFRs, masses, dust content etc., of Ly α emitters. These results were put in context by talks from theoreticians and local Universe observers. Comparisons with other classes of high redshift galaxies were also made. Emphasis was put on dedicated discussion sessions, summarised in this publication, where the current stand of observations were reviewed and discussions about what is most important to focus on in the future were held. The week comprised a three day conference with invited and contributed talks and a two day workshop with dedicated discussion sessions on pre-determined topics.

3 Conference overview

3.1 General overview

The conference week had 70 participants from four continents and thirteen countries. Of these 70 participants, 39 gave presentations and 17 presented posters. In total 28% of the oral presenters were female. The first three days of the conference were all devoted to the oral contributions; the first day with a theoretical theme starting with observations of $\text{Ly}\alpha$ in the local Universe and continuing with several theoretical talks on radiative transfer modeling and semi-analytic/hydro-dynamic simulations of the high redshift Universe. Following this, the second day was concerned with high redshift observations of $\text{Ly}\alpha$ emitters and what we know to date about the properties of LAEs at $z = 2 - 5$. The final conference day included two themes; first a session comparing the properties of high redshift LAEs to other types of high redshift galaxies, and secondly a session devoted to observations of so-called $\text{Ly}\alpha$ blobs. The two last days of the conference were in workshop style with in total six discussion sessions on *i)* new methods and selection methods, *ii)* morphology, *iii)* what can the local Universe observations tell us about the high redshift Universe?, *iv)* clustering, *v)* SED fitting and *vi)* $\text{Ly}\alpha$ blobs. Each discussion was chaired by one person who was asked to summarise the discussion in their session in this publication.

3.2 Highlights

In the first topic of the week, local Universe observations of $\text{Ly}\alpha$, the speakers lamented on the difficulty of UV observations of $\text{Ly}\alpha$. Not only do the observers have to see past the geocoronal $\text{Ly}\alpha$ emission which is very strong, and through the intergalactic reddening, there is also a lack of telescopes and instruments available for observations in the UV. From the few tens of objects observed to date, some conclusions were drawn. Firstly, from spectroscopic studies the conclusion was that the kinematics of the gas is very important for the observations of $\text{Ly}\alpha$, and that resolutions of better than 30 km s^{-1} are required to get a good handle on the line profile. This is important also for observations at high redshift. Imaging campaigns have shown that the escape fractions of $\text{Ly}\alpha$ in the local samples are low and that the $\text{Ly}\alpha$ emission does not necessarily resemble either the $\text{H}\alpha$ emission, nor the FUV. An interesting result is also the tentative result of an anti-correlation between the equivalent widths (EW) of $\text{Ly}\alpha$ and $\text{H}\alpha$, where the $\text{Ly}\alpha$ EW decreases with increasing $\text{H}\alpha$ EW.

In the second major topic of the week, theoretical models and predictions were presented. This topic could be broadly separated into three groups; radiative transfer

models, hydro-dynamical models and semi-analytical models. It was shown that radiative transfer models can fit the $\text{Ly}\alpha$ line profiles of LBGs (Lyman-break galaxies) very well. The models also show that the $\text{Ly}\alpha$ escape fraction of LBGs and LAEs mainly depends on the extinction of the IGM, and on the dust properties of the galaxies. LBGs intrinsically all have the same EWs, and the variations seen in observations all arise from varying column densities and dust properties. In his review talk, Ken Nagamine showed that two effects may control the appearance of LAEs; the escape fraction or the stochasticity (also known as duty cycle). In his hydro-dynamical models, the results favour a stochastic model rather than a model including only a constant escape fraction. Noteworthy is also a project put forward to try to understand the current day descendants of high redshift LAEs by looking at their counter-parts in the Millenium simulation. Finally, it was shown that clustering bias evolves rapidly with redshift and luminosity of LAEs, through results found with the semi-analytical model GALFORM.

In the large topic of observational results, the following points (among others) were made by various speakers:

- Especially for high redshift surveys ($z \gtrsim 4$) it is crucial to do spectroscopic follow-up of candidates as high EW interlopers with lower redshift are common. These interlopers are very similar in properties to LAEs.
- MUSYC is a large project to pin down the properties of $z \sim 3$ LAEs by various tests. Results show their candidates to be small, blue and young with signs of mergers. The AGN fraction is low.
- Tentative new results at $z \sim 2$ show evolution in the properties of LAEs from $z = 3 - 2$.
- The brightest LAEs always harbour AGN. A large fraction of LAEs are very young or have clumpy ISM based on comparisons of SFRs from UV and $\text{Ly}\alpha$.
- Field-to-field variations in properties of LAEs are still large even at areas of the order $\sim 0.2 \text{ deg}^2$.
- The $\text{Ly}\alpha$ EWs of LAEs may be boosted by dust absorption of UV continuum photons.
- The specific star formation rates of LAEs are the highest of all high redshift galaxy populations.

Following the observational results came a series of talks comparing LAEs to other populations of galaxies. Several speakers indicate that LBGs and LAEs share many properties, especially if limited to the same luminosity ranges. Perhaps an LBG is a later stage of an LAE? LBGs with $\text{Ly}\alpha$ emission are bluer than those without $\text{Ly}\alpha$ emission, and there appears to be a lack of massive LBGs with $\text{Ly}\alpha$ emission. The properties of LBGs, such as luminosity and number density, appears to evolve strongly with redshift. Two talks mentioned $\text{Ly}\alpha$ emission in the context of gamma-ray burst (GRB) host galaxies and sub-millimeter galaxies (SMGs). Earlier results had indicated that all GRB host galaxies had $\text{Ly}\alpha$ emission, but the results from a new large project showed that only $\sim 22\%$ have detectable $\text{Ly}\alpha$ emission.

In the final session, so-called Ly α blobs (LABs) were discussed. The largest sample to date is that found in the SSA22 region by Yuichi Matsuda and collaborators. Of their sample, 28% have been spectroscopically confirmed and 19% have $EW_0 > 100 \text{ \AA}$. Results show that the size, surface brightness and luminosity distributions are all continuous from LAEs to LABs, indicating that they are part of the same underlying population. LABs are however of the order 100 – 1000 times less abundant than LAEs. A new way of finding LABs through broad-band imaging was presented. Five blobs had been found to date with this method, including one with strong He II emission. In several talks the powering mechanisms behind the extended Ly α emission were discussed with arguments in favour of AGN scenarios (based on X-ray and sub-mm detections), extreme star formation scenarios (based on mid-IR and PAH detections) and cooling radiation (based on He II emission). It is clear that the question of LAB emission mechanisms is not solved yet.

3.3 Concluding remarks

We enjoyed organising this conference and found the scheduling of long coffee and lunch breaks, aiming to encourage discussions in informal groups, especially positive. It became clear from the meeting that this topic of research is a booming industry with many young scientists getting involved. It was also clear that the early days of this science when individual objects were presented in publications are being replaced by larger samples and an altered view from being mainly about *detection* to being more about *analysis* and *conclusions*. This is a pivotal and highly interesting time to work with Ly α selected galaxies and many fascinating results are to be expected in the next ten years.

4 Acknowledgements

This conference was organised by the SOC consisting of Johan Fynbo, Eric Gawiser, Klaus Meisenheimer, Kim Nilsson (chair), Daniel Schaerer and Göran Östlin, and the LOC consisting of Helmut Dannerbauer, Jaron Kurk, Kim Nilsson (chair), Heide Seifert and Christian Tapken. Further, we wish to thank the financial contributors; the Max Planck Institute for Astronomy in Heidelberg and the DFG / Sonderforschungsbereich. Finally, a big thank you to all the participants, contributors and discussion leaders for the enthusiastic participation. The presentations of all contributions can be found at <http://www.mpia.de/Public/Aktuelles/Tagungen/lae08/lae08.html>.

References

- Cowie, L.L., & Hu, E.M., 1998, *AJ*, 115, 1319
- Davé, R., Finlator, K., & Oppenheimer, B.D., 2006, *MNRAS*, 370, 273
- Deharveng, J.-M., Small, T., Barlow, T.A., et al., 2008, *ApJ*, 680, 1072
- Dey, A., et al. 2005, *ApJ*, 629, 654
- Fardal, M. A., Katz, N., Gardner, J. P., Hernquist, L., Weinberg, D. H., & Davé, R. 2001, *ApJ*, 562, 605
- Francis, P.J., Palunas, P., Teplitz, H.I., Williger, G.M., & Woodgate, B.E., 2004, *ApJ*, 614, 75
- Furlanetto, S., Schaye, J., Springel, V., & Hernquist, L., 2005, *ApJ*, 622, 7
- Fynbo, J.U., Møller, P., & Warren, S.J., 1999, *MNRAS*, 305, 849
- Fynbo, J.U., Møller, P., & Thomsen, B., 2001, *A&A*, 374, 443
- Fynbo, J.P.U., Møller, P., Thomsen, B., et al., 2002, *A&A*, 388, 425
- Fynbo, J.P.U., Ledoux, C., Møller, P., Thomsen, B., & Burud, I., 2003a, *A&A*, 407, 147
- Fynbo, J.P.U., Jakobsson, P., Möller, P., et al., 2003b, *A&A*, 406, L63
- Gawiser, E., Francke, H., Lai, K., et al., 2007, *ApJ*, 671, 278
- Haiman, Z., Spaans, M., & Quataert, E. 2000, *ApJ*, 537, L5
- Iye, M., Ota, K., Kashikawa, N., et al., 2006, *Nature*, 443, 186
- Kobayashi, M.A.R., Totani, T., & Nagashima, M., 2007, *ApJ*, 670, 919
- Kunth, D., Leitherer, C., Mas-Hesse, J.M., Östlin, G., & Petrosian, A., 2003, *ApJ*, 597, 263
- Laursen, P., Razoumov, A.O., & Sommer-Larsen, J., 2009, submitted to *ApJ*, arXiv:0805.3153
- Le Delliou, M., Lacey, C., Baugh, C.M., et al., 2005, *MNRAS*, 357, L11
- Le Delliou, M., Lacey, C., Baugh, C.M., & Morris, S.L., 2006, *MNRAS*, 365, 712
- Mao, J., Lapi, A., Granato, G.L., de Zotti, G., & Danese, L., 2007, *ApJ*, 667, 655
- Nagamine, K., Ouchi, M., Springel, V., & Hernquist, L., 2008, arXiv:0802.0228
- Nilsson, K. K., Fynbo, J. P. U., Møller, P., Sommer-Larsen, J., & Ledoux, C. 2006, *A&A*, 452, L23
- Nilsson, K.K., Tapken, C., Møller, P., et al., 2009, *A&A* in press, arXiv:0812.3152
- Orsi, A., Lacey, C.G., Baugh, C.M., & Infante, L., 2008, Accepted in *MNRAS*, arXiv:0807.3447
- Ouchi, M., Shimasaku, K., Akiyama, M., et al., 2008, *ApJS*, 176, 301
- Pentericci, L., Kurk, J.D., Röttgering, H.J.A., et al., 2000, *A&A*, 361, L25
- Smith, D. J. B., & Jarvis, M. J. 2007, *MNRAS*, 378, L49
- Stiavelli, M., Scarlata, C., Panagia, N., et al., 2001, *ApJ*, 561, L37
- Tasitsiomi, A., 2006, *ApJ*, 645, 792
- Van Breukelen, C., Jarvis, M.J., & Venemans, B.P., 2005, *MNRAS*, 359, 895
- Venemans, B.P., Röttgering, H.J.A., Miley, G.K., et al., 2007, *A&A*, 461, 823
- Verhamme, A., Schaerer, D., & Maselli, A., 2006, *A&A*, 460, 397
- Weidinger, M., Møller, P., Fynbo, J.P.U., & Thomsen, B., 2006, *A&A*, 436, 825
- Östlin, G., Hayes, M., Kunth, D., et al., 2008, submitted to *AJ*, arXiv:0803.1174

New Methods and Selection Methods

Daniel Kunth,^a Guillermo A. Blanc,^b Michael Rauch^c
& Paolo Cassata^d

^a*Institut d'Astrophysique de Paris, Paris, France*

^b*Astronomy Department, University of Texas at Austin, USA*

^c*Observatories of the Carnegie Institution of Washington, USA*

^d*Astronomy Department, University of Massachusetts, Amherst, MA 01002, USA*

Abstract

As the topics of study of Ly α emitters evolve, new selection methods are being developed to find these high redshift galaxies. In this proceedings, three new methods are presented, based on large integral field unit spectrographs, ultra-deep slit spectroscopy and serendipitous discoveries.

Key words:

conference proceedings, observational cosmology, Ly α emitters, high redshift galaxies

PACS: 98.80.Es

1 Introduction

Traditionally, Ly α emitters (LAEs) have been detected mainly with narrow-band imaging, with additional galaxies detected in spectroscopy with or without slits. The advantage with the narrow-band approach is that large areas may be covered in relatively little observing time. The disadvantages are that the surveys are relatively shallow, and that follow-up spectroscopy is needed to confirm the line and its identification. Spectroscopy, on the other hand, gives a direct confirmation and can reach faint magnitudes, but surveys very small volumes at a time and is therefore very time consuming. Accordingly, considering the progress and the interest in the topic of Ly α emitter studies, it is timely to think of new selection methods for emission-line galaxies. We here present three new methods in development; those of using large integral field unit (IFU) spectrographs (sec. 2), observing to very faint fluxes in single slit spectroscopy (sec. 3) and LAEs as by-products in large spectroscopic surveys (sec. 4).

2 The VIRUS-P Pilot Survey for Lyman Alpha Emitters at $2 < z < 4$: First Results (G.A. Blanc)

We present the first results of a blind search for Lyman Alpha Emitters in the $1.9 < z < 3.8$ range with the VIRUS-P integral field spectrograph on the 2.7m Harlan J. Smith telescope at McDonald Observatory. We obtained spatially resolved spectroscopy over an area of $\sim 114 \text{ arcmin}^2$. In this work we present the analysis of a subsample of the data covering $\sim 40 \text{ arcmin}^2$ on the central region of the COSMOS field, where we have detected 45 LAEs and 10 ambiguously classified objects consistent with being LAEs to a flux limit of $\sim 6 \times 10^{-17} \text{ ergs s}^{-1} \text{ cm}^{-2}$. Spectra and images of the optical counterparts of these objects can be found in the Power Point presentation available at the conference website. The extremely large $1.9' \times 1.9'$ field of view of VIRUS-P together with its 3550-5850 Å wavelength coverage allows us to survey the Lyman Alpha line over a comoving volume of 21000 Mpc^3 in a single pointing, this is a 50 times larger volume per area on sky than the one sampled by typical narrow-band surveys.

The observed redshift distribution of LAEs is in agreement with an scenario of no evolution of the $\text{Ly}\alpha$ luminosity function from $z \sim 4$ to $z \sim 2$. Although the current low number of objects and uncertainties in spectral classification do not allow us to discern significantly between different evolution models, this will be possible after the pilot survey is completed.

VIRUS-P is the prototype instrument for VIRUS, a massively replicated integral-field spectrograph consistent in 145 units like VIRUS-P, which will be installed on the 9.2m Hobby-Eberly Telescope. With VIRUS we will be able to produce a sample of $\sim 1,000,000$ LAEs which will allow us to map the large scale structure of the universe at high redshift in order to set constraints in the evolution of the Dark Energy equation of state through baryonic acoustic oscillations (BAO) as part of the Hobby-Eberly Telescope Dark Energy Experiment (HETDEX, www.hetdex.org).

The pilot survey will continue for the next few months in order to better constrain the properties of LAEs in preparation for HETDEX. We expect to produce a final sample of ~ 200 LAE over an area of $\sim 150 \text{ arcmin}^2$. This sample will allow us to study the evolution of the $\text{Ly-}\alpha$ luminosity function in the $2 < z < 4$ range, select $z \sim 2$ LAE for $\text{H}\alpha$ follow-up at NIR wavelengths, and characterize the stellar populations in these objects as a function of redshift using SED fitting.

3 Ultra-Deep Surveys for Lyman α Emitters at Redshift ~ 3 (M. Rauch)

Theory predicts that a number of physical effects can illuminate the distribution of neutral hydrogen in the universe by means of the hydrogen Lyman α line. The UV

radiation from star-formation may induce galactic Lyman α emission; more massive galactic halos may produce visible cooling radiation; the most tenuous large scale structure in HI may glow in Lyman α fluorescence, caused when extragalactic UV background continuum photons impinge on optically thick hydrogen clouds and filaments.

A search for this latter effect, using a 92 hour long spectroscopic long slit exposure with the ESO VLT FORS2 instrument, while failing to detect the desired signal, uncovered a surprising number of brighter, single line sources, probably to be identified with stellar induced Lyman α emitters at redshift 3. With a number density of $\sim 3 \times 10^{-2} \text{ Mpc}^{-3}$ the sources are 25 times as numerous as Lyman break galaxies, according to the usual definition, or as the relatively bright Lyman α emitters surveyed by typical narrow-band surveys discussed at the present workshop. Mapping the new population of emitters onto the mass function of dark matter halos, their large number density requires them to correspond to halos with masses as low as a few times $10^{10} M_{\odot}$, or virial velocities as low as 50 kms^{-1} . In other words, we appear to be getting a first glimpse of dwarf galaxies at high redshift. Our finding of such a large number density of objects, together with the mostly extended nature of their Lyman α emitting regions, suggests that the covering factor of the sky by detectable Ly α emission is similar to the rate of incidence of Damped Ly α absorption systems. The latter are the still mysterious reservoir of neutral hydrogen at high z , and were in fact the first candidates for high redshift galaxies ever detected. We propose that our new population of Ly α emitters may be the host galaxies of damped Ly α systems, a suggestion that reconciles many observational limits on damped Lyman α systems with the likely properties of a population of numerous, low mass, gas-rich, dust-poor, and weakly star-forming dwarf galaxies.

We have outlined future research, including further spectroscopic surveys in regions with deep, space-based imaging like the Hubble Deep Fields, that may shed light on the connection between Lyman α emitters, and Lyman break galaxies, and thus the local star formation rate.

So far our observations have shown that spectroscopy of blank fields with large ground based telescopes is directly competitive with the deepest images from space. Given a substantial, but not unusual investment in observing time we may be able to reach depths in probing high redshift galaxies never reached before with any observational technique.

4 Star Formation Density at $2 < z < 6.5$ from Lyman Alpha Emitters in VVDS (P. Cassata)

Vimos VLT Deep Survey (VVDS) collected spectra for about 8000 galaxies with $m_i < 24$ (deep survey) and for about 1200 galaxies with $m_i < 24.75$ (ultradeep

survey). Since the slits used for the spectroscopy are extended ($1 \times 4 \div 12$ arc-sec), these datasets can be used to search for Ly α emitters. In fact, if a Ly α galaxy serendipitously falls in a slit, the Ly α line will appear in the 2-d spectrum. Actually, the sky area covered is significant, and the very long integration times allow to reach very low Ly α fluxes. In particular, deep survey slits cover an effective area on the sky of 22.5 arcmin^2 , the red grism gives a wavelength range between 5500 and 9200 Å (so giving a redshift range $3.5 < z < 6.7$), and the integration time of 16200 seconds allows to detect Ly α lines down to fluxes of about $\sim 5 \times 10^{-18} \text{ erg cm}^{-2} \text{ s}^{-1}$. On the other hand, ultra-deep slits cover 3.5 arcmin^2 , the blue and red grisms produce a wavelength range between 3000 and 9200 Å (giving a redshift range $2 < z < 6.7$), and the longer exposure time (65000 s.) allows to reach line fluxes of $\sim 1.5 \times 10^{-18} \text{ erg cm}^{-2} \text{ s}^{-1}$.

We carefully estimated the sample completeness, as a function of redshift and luminosity, making use of Monte Carlo simulation. Moreover, we estimated the average slit flux loss: since the galaxies in our sample just serendipitously fall inside the slits, they are not expected to be perfectly centered in the slits.

Finally, we assembled a sample of 138 serendipitous Ly α emitters, and we also added 66 targets of the VVDS Ultra-deep survey that turned out to be Ly α emitters. The final sample contains 203 emitters, with redshift between $z = 2$ and $z = 6.7$, with a median redshift $\langle z \rangle = 3.5$ and 5 candidates at $z > 6.3$. Up to date, this sample is one of the largest Ly α emitters sample with confirmed spectroscopic redshift.

Thanks to the very long exposure times, we could reach luminosities as low as $L_{\text{Ly}\alpha} = 10^{41}$, and our sample is 50% complete at $L_{\text{Ly}\alpha} = 10^{41}$ and $z < 3$. Thus, we can carefully measure, at $2 < z < 3$, the slope of the faint end of the luminosity function. This is very important, since up to now the bulk of the Ly α samples in literature do not reach such low luminosities and thus can not constrain this slope. We find that actually the faint end of the Ly α luminosity function is very steep: we obtain in fact a parameter $\alpha \sim -1.7$.

The luminosity functions of Ly α galaxies appear to be consistent with no evolution from $z = 6$ to $z = 2$. As a consequence, if we simply assume the classical Kennicutt law to convert Ly α luminosities to star formation rates, we obtain a roughly constant contribution of the Ly α galaxies to the global star formation rate of the universe: we find $\sim (9, 8, 7, 10) \times 10^{-3} M_{\odot} \text{ yr}^{-1} \text{ Mpc}^{-3}$ respectively at $z = 2.5, 3.8, 4.3, 6$.

For more details, see the Powerpoint presentation in the conference website.

Morphologies of Ly α –Emitting Galaxies

Nicholas Bond

Department of Physics and Astronomy, Rutgers University, Piscataway, NJ., USA

Abstract

Lyman Alpha Emitters (LAEs) are high-redshift galaxies that are believed to be actively star-forming and low in mass. Although such a population of galaxies would not be expected to lie on the Hubble Sequence, there is much we can learn from their morphological properties, including the size and distribution of their star-forming regions, the spatial correlation between emission in different bandpasses, and the possible presence of a merger/interaction with one or more neighboring galaxies. Early morphological studies suggest that most LAEs are small in size ($\lesssim 1$ kpc) and concentrated, but some (~ 20 –45%) are seen to display clumpy/irregular morphologies extending over larger radii. Constructing a more detailed picture will require a standard set of depth-independent morphological diagnostics for high-redshift galaxies. These diagnostics can then be measured differentially with redshift, shedding light on the evolution of the galaxy formation *process* with time.

Key words:

It is generally agreed upon that LAEs at high redshift are actively star-forming (e.g. Cowie & Hu, 1998), low in mass (Gawiser et al., 2007), and low in dust (e.g. Venemans et al., 2005). Although such a population of galaxies would not fit cleanly into any existing classification scheme, there is still much we can learn from their morphological properties. In this proceedings, I will summarize the current state of our knowledge of LAE morphologies, including some results from low-redshift star-forming galaxies, and then go on to discuss the future direction of the field, putting emphasis on the need for a standard set of morphological diagnostics for high-redshift galaxies. Throughout this proceedings, we will assume a concordance cosmology with $H_0 = 71 \text{ km s}^{-1} \text{ Mpc}^{-1}$.

1 What We Know

The effort to measure the morphologies of LAEs is still in its earliest stages, with most of the existing results being reported in the broadband rest-frame

ultraviolet. There are currently no published studies of LAE morphologies in the Ly α narrowband filter, but at least two are in preparation (?). When interpreting the latter, it will be important to have a standard for comparison at low redshift.

1.1 Morphologies of Star-Forming Galaxies at Low-Redshift

Östlin et al. (2008) present six Ly α images of $z \sim 0$ star-forming galaxies, selected to cover a range in luminosity and metallicity. They find a wide variety of Ly α morphologies, the properties of which depend primarily on the spatial distribution and kinematic properties of the interstellar media of the underlying galaxies. There is no obvious correlation, in general, between the Ly α , H α , and broadband far-ultraviolet morphologies, but there is a tendency for Ly α to appear in a diffuse halo surrounding the galaxy. This halo is thought to be a consequence of resonant scattering in the Ly α line and can act to "smear" the narrowband morphology relative to the distribution of star-forming regions in the galaxy.

1.2 Morphologies of High-Redshift Galaxies

The qualitative morphological properties of the "typical" LAE are generally agreed upon, though "typical" objects only make up a slim majority of the existing samples. At $3 \lesssim z \lesssim 6$, most LAEs are small (generally < 1 kpc), compact ($C > 2.5$), and barely resolved at HST resolution (Venemans et al., 2005; Pirzkal et al., 2007; Overzier et al., 2008). However, many ($\sim 20 - 45\%$) have also been found that are clumpy or irregular, with components extending to several kiloparsecs. The clumpy objects are generally treated separately and given only crude, qualitative descriptions. In addition, preliminary attempts to fit the LAE light profiles have yielded a wide range of Sersic indices, with a preference for $n \lesssim 1$ (Gronwall et al., 2009, in prep.; Bond et al., 2009, in prep.).

2 Challenges

There are many difficulties involved in performing a morphological analysis of LAEs, but perhaps the greatest difficulty of all is deciding which analysis to perform. The Hubble Sequence has long been the golden standard for classification of low-redshift galaxies, but there is no evidence that this scheme applies at $z \gtrsim 2$ (Dickinson, 2000). Furthermore, deep observations of LAEs

are typically taken in the rest-frame ultraviolet, in which the morphologies of even low-redshift galaxies will be clumpy and more difficult to classify. Given the low signal levels in existing images of LAEs and the likely "disorganized" nature of many of these objects, it would be premature to develop a new classification scheme. Nevertheless, any set of morphological parameters that, 1) can be measured *differentially* over a wide range of redshifts and, 2) is not sensitive to the depth of the observations, would be useful to report to the high-redshift galaxy community.

The latter requirement, that the morphological parameters be insensitive to depth, is not trivially satisfied by many of the standard measures. For example, the asymmetry parameter (from the CAS scheme, Conselice, 2003) has been seen to change dramatically between observations of individual LAEs in the GEMS (Rix et al., 2004) and the deeper GOODS (Giavalisco et al., 2004) survey (Gronwall et al., 2009, in prep.). Such a depth dependence would also be expected in any parametric fit to a model that is a poor description of the true light distribution (as, for example, the Sersic profiles may be).

3 Future

3.1 Methodology

The most frequently reported LAE morphological parameter has, so far, been the half-light radius, but care needs to be taken when reporting even this simple quantity. The most direct (and model-independent) way of measuring it is with a stellar photometry code, such as SExtractor (Bertin & Arnouts, 1996), which will simply look for the radius of a circular aperture within which half of the light is detected. Another method, which yields a result closer to the intrinsic half-light radius of the LAE, is to use a profile-fitting code, like GALFIT (Peng et al., 2002). Developed for the fitting of well-resolved low-redshift galaxies, GALFIT convolves a model light profile with the point spread function and minimizes χ^2 over a chosen set of model parameters. Although this technique allows for the fitting of half-light radii smaller than the resolution limit (as with many LAEs), the user must assume a profile shape in order to perform the fits. If the LAE population does not follow the assumed profile, one cannot make a meaningful comparison of best-fit parameters between samples observed at different depths.

We know very little about the intrinsic light profiles of LAEs, so a better approach would be to use *non-parametric* measures, such as the Gini coefficient, which quantifies the relative frequency of flux values within the source pixels, and M_{20} , which is the second-order moment of the 20% brightest pixels

(Lotz, Primack, & Madau, 2004). These measures have already been applied to LBG data-sets (Lotz et al., 2006), though there are some questions as to their usefulness at low signal-to-noise (Lisker, 2008).

Further complicating estimates of the half-light radius distribution are the "clumpy" LAEs. Even at low redshift, ordinary late-type galaxies can look clumpy in the UV, so there is ambiguity in treating individual clumps. Are they all part of a single galaxy or are they separate objects in the process of merging? Current estimates of the half-light radius distribution indicate a strong preference for sub-kpc radii, but this generally excludes objects found to have complex morphologies. Could these "clumpy" objects fill in a continuum between the barely-resolved LAEs and the more extended Lyman Alpha blobs? Larger high-resolution samples (preferably in the Ly α narrowband) will be needed in order to answer this question.

Another possibility is to measure simple morphological quantities differentially with *wavelength* within a given object. For example, one could compare the offsets between the centroid in Ly α and that in the far-UV or rest-optical. This has the advantage that, with good astrometry, it can be done with ground-based imaging, but again, the presence of an extended Ly α halo could make it a depth-dependent quantity.

3.2 Observations

If we wish to obtain a more complete understanding of the physical nature of LAEs, future observations will need to more completely sample their emission. Optimally, we would have deep, space-based observations of LAEs in a wide range of rest-frame wavebands, including Ly α , H α , UV, optical and even near-infrared for the lowest redshift galaxies. High-resolution images in Ly α will allow us to map the emission we detect from the ground and should provide insight into what actually drives the Ly α emission. Rest-frame optical images, on the other hand, will provide a smoother and more complete map of the stellar populations within these galaxies and allow us to more directly compare them to objects we see at $z \sim 0$. At present, we are working primarily with UV images which, in isolation, provide relatively little information about the underlying galaxy. Directly imaging some of these objects in Ly α and the rest-optical should be a high priority.

4 Conclusions

At present, there are no underlying physical theories that we can use as a basis for our observations of LAE morphologies, so we must provide the body of knowledge needed to begin formulating such a theory. To this end, consistency is essential, and we should work to ensure that the diagnostics we choose can be compared between observations made at different depths and at different redshifts. Furthermore, lacking an obvious standard for comparison in the local universe, these diagnostics should be measured *differentially* as a function of redshift if we wish to begin to form a picture of how the galaxy formation process has evolved with time.

References

- Bertin, E., & Arnouts, S., 1996, A&A, 117, 393
Gawiser, E., Francke, H., Lai, K., et al., 2007, ApJ, 671, 278
Conselice, C.J., 2003, ApJS, 147, 1
Cowie, L.L., & Hu, E.M., 1998, AJ, 115, 1319
Dickinson, M., 2000, in Philosophical Transactions of the Royal Society of London, Series A, 358, 2001
Giavalisco, M., Ferguson, H.C., Koekemoer, A.M., et al. 2004, ApJL, 600, L93
Lisker, T., 2008, ApJS, 179, 319
Lotz, J.M., Madau, P., Giavalisco, M., Primack, J., & Ferguson, H.C., 2006, ApJ, 636, 592
Lotz, J.M., Primack, J., & Madau, P., 2004, AJ, 128, 163
Overzier, R.A., Bouwens, R.J., Cross, N.J.G., et al., 2008, ApJ, 673, 143
Peng, C.Y., Ho, L.C., Impey, C.D., & Rix, H.-W., 2002, ApJ, 124, 266
Pirzkal, N., Malhotra, S., Rhoads, J.E., & Xu, C., 2007, ApJ, 667, 49
Rix, H.-W., Barden, M., Beckwith, S.V.W., et al., 2004, ApJS, 152, 163
Venemans, B.P., Röttgering, H.J.A., Miley, G.K., et al., 2005, A&A, 431, 793
Östlin, G., Hayes, M., Kunth, D., et al., 2009, astro-ph/0803.1174

What can Lyman α observations of nearby galaxies tell us about the high redshift Universe?

Göran Östlin

*Department of Astronomy, Stockholm University, AlbaNova university center,
SE-106 91 Stockholm, Sweden*

Abstract

This discussion session started off with a quick review of some key results regarding Ly α emitters (LAEs) at low redshift: some illustrative images were shown, some intriguing results highlighted, and some comparison with high redshift LAEs made. Then followed an open discussion for about one hour which touched upon questions such as: how similar are low- and high- z objects, Ly α escape fractions, what observations are needed to go from interesting to understandable results on low- z objects, how do we understand the complexity of Ly α in local galaxies and what does it imply for high- z objects?

Key words:

PACS:

1 Introduction

Being a resonant line Lyman α (Ly α) becomes optically thick even at modest column densities. If embedded in a static neutral hydrogen cloud, Ly α photons will have a short mean free path and must experience multiple scatterings, every time with the risk of being destroyed by dust, before it can get out – one may say that the Ly α photons are *resonantly trapped*. Hence, Ly α radiative transport through and escape (or not) from a galaxy is a complex problem, compared to e.g. H α .

The potential power of Ly α for high redshift studies comes from the combination of its intrinsic strength and a rest wavelength that makes it accessible for observations in the optical atmospheric transmission window for redshifts from $z \sim 2 - 7$. This was realized already in the sixties (Partridge & Peebles

1967), and despite a slow start, during the last decade large numbers of high- z LAEs have been found, mainly through narrow band imaging (e.g. the talk by Hu at this workshop). The occurrence of this conference is a testimony of this success.

Local Universe studies, on the other hand, need access to the ultra-violet (UV) domain and hence only space based observations are possible. Consequently, many fewer studies of the Ly α emission from local sources have been performed as compared to high redshifts. While difficult to obtain, low- z Ly α observations has some vital advantages: spatial resolution and easier access to data at other wavelengths. Another effect of a smaller distance is of course that apparent fluxes are higher than for (equal luminosity) high- z sources, and there is moreover not much of cosmological surface brightness dimming; but the need to go to space and less powerful instrumentation partly offsets these particular advantages. The spatial resolution is both a blessing and a challenge: for spectroscopy, in the absence of space-flown UV Integral Field Units, it results in detailed studies of very small physical regions. Imaging can give us more of the full picture, at the price of spectral information. This is the usual trade of spectral and spatial resolution, but particularly for Ly α having both is important since the radiative transport both displaces the emission and affects the line shape.

While the expansion of the Universe shifts Ly α into the optical window, it shifts a large amount of other useful spectral information to wavelengths where they cannot easily be observed, especially at very high redshifts. At moderate redshift, cosmological dimming is smaller and the rest-frame optical emission can still be accessed in the near IR. Hence, more information can be extracted from the individual LAEs which can be used to aid our understanding of the astrophysics of LAEs at high redshifts. This has been part of the rationale for this conference.

2 Some key results from the local Universe

Spectroscopy:

Most of the early Ly α observations of sources in the local Universe were made with the International Ultraviolet Explorer (IUE), which obtained integrated low resolution spectra through a large (~ 20 arcsec) aperture, see e.g. Charlot & Fall (1993) and Giavalisco et al. (1996). With the Hubble Space Telescope (HST) it became possible to obtain high resolution spectra through smaller apertures. HST has resolved the Ly α line profiles but is in most cases restricted to the brightest knots of the starburst. If there is one result which stands out then it must be the apparent importance of the neutral ISM kinematics. Whenever Ly α has been seen in emission, blueshifted ISM absorption lines

have also been observed (Mas-Hesse’s talk at this conference, see also Kunth et al. 1998, Mas-Hesse et al. 2003).

Related to this was the apparent and surprising *unimportance* of dust and/or metallicity as illustrated by I Zw 18 and SBS 0335–052, the most metal-poor star forming galaxies known in the local Universe, turning out to be damped *absorbers*. Caution is necessary though, since the number of objects is small (see also Giavalisco et al. 1996).

A model based on the hydrodynamical evolution of an HII-region with an expanding super-bubble could explain these observations (Mas-Hesse et al. 2003). In simple words, this model says that it is not until feedback from stellar evolution has accelerated the surrounding ISM that Ly α can escape, the relative velocity shift then allowing Ly α to avoid the resonant trapping in H I.

Imaging:

The suspicion that some or all of the Ly α may resonantly scatter out of the spectroscopic apertures motivated an attempt at Ly α imaging with HST of a local sample of star forming galaxies. The results obtained paint a complex and yet (due to the small number of targets) very incomplete, picture (Hayes et al. 2007, Östlin et al. 2009). A striking example of an image of a local starburst galaxy is shown in Fig 1, which is an RGB composite of H α (red), UV-continuum (green) and Ly α (blue).

Spatially, Ly α is only weakly correlated with the UV continuum and H α . Even those galaxies that do emit Ly α display several absorption holes, notably towards young UV-bright regions. The bulk of Ly α comes out at low UV surface brightness, far from the ionizing sources. This means that Ly α transport and escape from a galaxy is primarily governed by resonant scattering. Therefore is Ly α imaging a necessary complement to high spectral and spatial resolution spectroscopy in order to “get the full picture”. Two strong Ly α absorbers have been studied but results are inconclusive – one yielded net absorption and the other weak emission.

Ly α and H α equivalent widths have been found to be anti-correlated, see Fig. 2. This is unexpected in spectral evolutionary synthesis models, but compatible with the super-wind model quoted above.

Escape fractions are small (from zero to 15%) and cannot be explained by standard reddening corrections, see also Fig. 2.

Subtracting the continuum from HST Ly α images is non-trivial (Hayes et al. 2009). The instrument configuration, but also the strong evolution of the spectrum near Ly α causes this. Although the effects are usually smaller at high- z ,

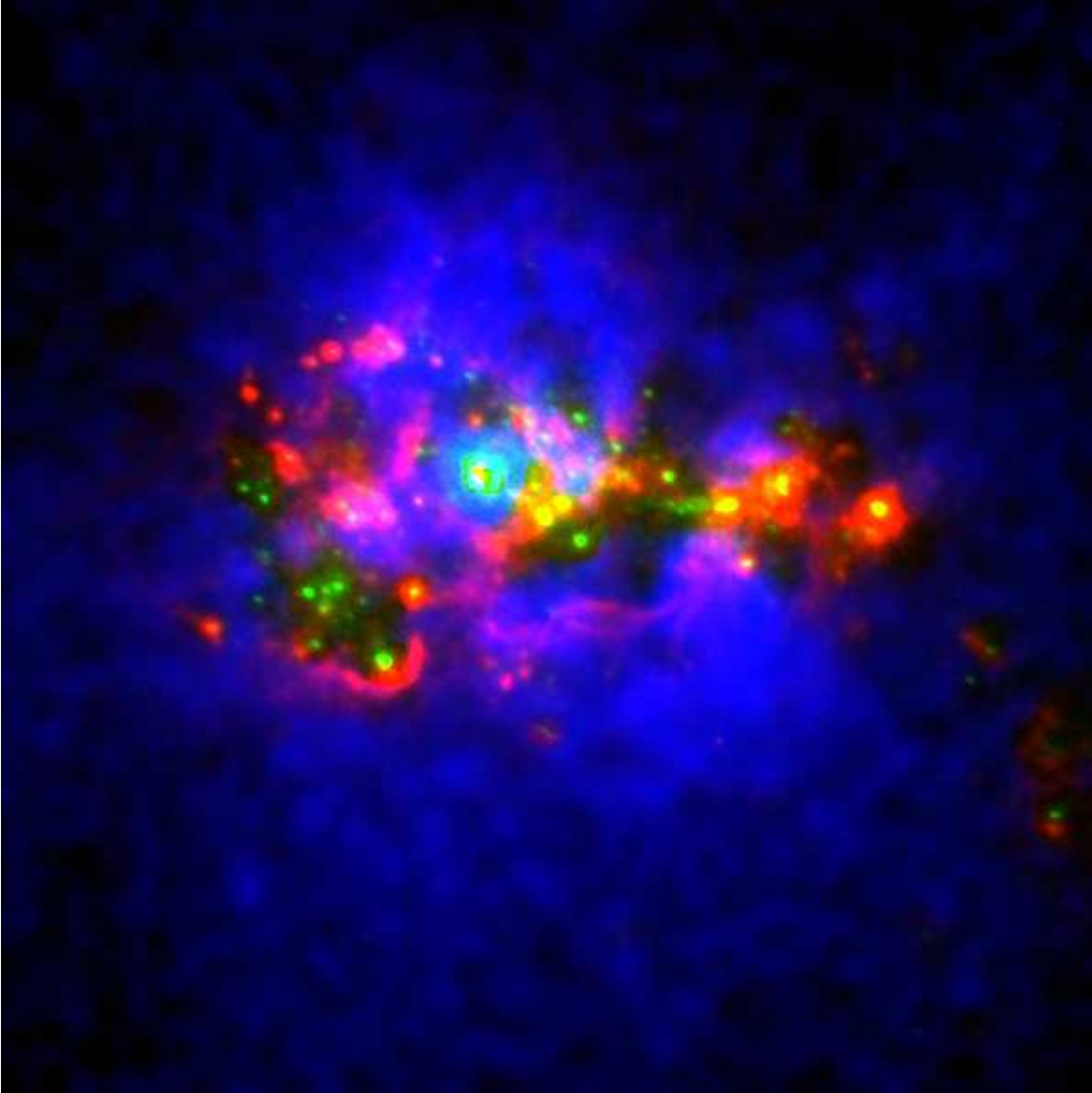


Fig. 1. RGB composite of $H\alpha$ (red), UV-continuum (green) and $Ly\alpha$ (blue) of the 38 Mpc distant, metal-poor, dwarf starburst galaxy ESO 338-04. The size of the image is 20×20 arcsec, or 3.5×3.5 kpc. $Ly\alpha$ emission is not dominated by the bright super star clusters (SSCs) that dominate the production of ionizing photons. Towards most of them, $Ly\alpha$ is rather seen in absorption. The starburst region shows both emission and absorption regions resulting from ISM porosity or the velocity structure of the neutral ISM. Most of the escaping $Ly\alpha$ emission comes from a diffuse extended component where $Ly\alpha/H\alpha \gg 10$, that can only be produced by resonant scattering (Östlin et al. 2009).

they may in many cases require considerations and could cause overestimates of $EW(Ly\alpha)$ (see Hayes et al. 2006).

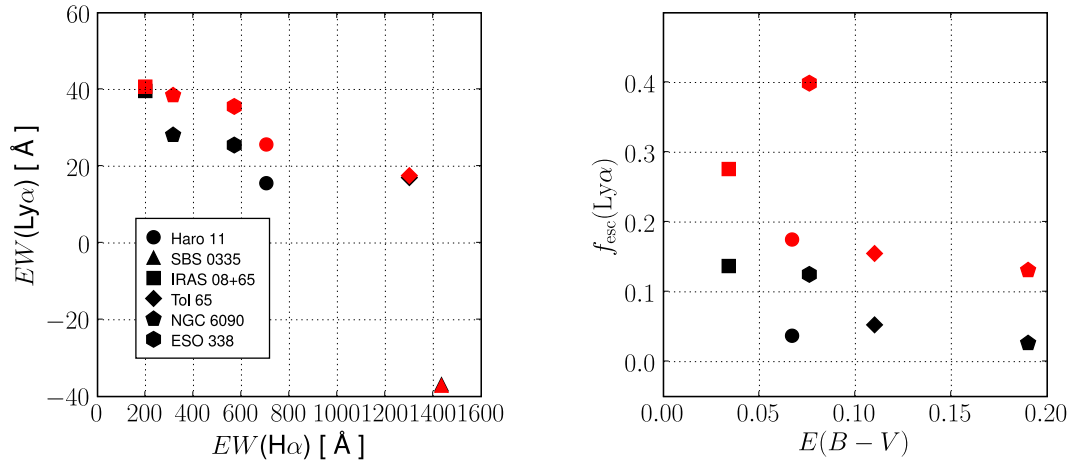


Fig. 2. **Left:** equivalent width of $H\alpha$ vs. $Ly\alpha$ for the sample in Östlin et al. (2009) (also the talk of Hayes at this conference). Black symbols are observed escape fractions, whereas red/grey symbols are values where $Ly\alpha$ has been corrected for reddening. **Right:** $Ly\alpha$ escape fraction vs. reddening. Black symbols are observed escape fractions, whereas red/grey symbols are values where $Ly\alpha$ has been corrected for reddening. If standard reddening applied, then this exercise should render all red/grey points equal to unity. The fact that they are not shows that simple extinction corrections do not work (see also Atek et al. 2008).

3 Discussion

– Are low- z $Ly\alpha$ galaxies fundamentally different from high- z ones?

$Ly\alpha$ emitters do not reflect a physical class of objects, but a selection method. This selection function cannot be reproduced at low z , making direct comparisons difficult. At this conference it was indeed discussed (talks by Gawiser viz. Fynbo) whether LAEs should be viewed as a special class of galaxy or just a (transient) property.

In terms of $Ly\alpha$ equivalent widths it may seem that low- z $Ly\alpha$ galaxies are different from high- z ones, but in terms of overall UV luminosity, and UV luminosity vs. $EW(Ly\alpha)$, four of the six local sources imaged in $Ly\alpha$ fall in the range of LAEs and LBGs (see Gronwall et al. 2007, Verhamme et al. 2008, Ouchi et al. 2008).

Further, at high- z , the EW distribution is highly skewed towards low EW objects and the lack of high EW local objects could be a consequence of different selection function and the small number of objects studied yet. Are there objects in the local Universe with $EW(Ly\alpha)$ which have so far evaded observers? How would we find them?

In the not too distant Universe ($z \sim 0.3$) LAEs have been detected through slitless spectroscopy with the GALEX satellite. Most of these LAEs have modest EWs but the sample size is also smaller than at high- z . Although technically different from most high- z selections, the luminosity function of the $z \sim 0.3$ objects suggest that escape fractions were higher at high- z (Deharveng et al. 2008).

If the super-wind model, originating from the high-resolution spectroscopy results for local galaxies (and still compatible with the imaging results) is correct and applies also at high- z (see e.g. Shapley et al. 2003), we should not expect to see LAEs with very high equivalent widths, since when the starburst is sufficiently evolved (e.g. at least 5 Myr) to have accelerated the ISM, the intrinsic Ly α EW will have dropped by a factor of several. This is contrary to observations, hence some other mechanism must be at play as well. If star formation is extended in time, so that the first generation of stars in a starburst can clear the paths and accelerate the ISM for Ly α from the next one, high EWs could result. For instance, the predicted EW for a constant SFR at 10 Myr is about 150 Å.

The ISM and dust geometry/distribution is another key factor: if dust is confined to discrete HI clouds, Ly α will scatter off their surfaces while the UV continuum has to penetrate through, resulting in higher net losses, and hence higher EWs (Neufeld 1991, and Finkelstein's talk at this workshop). Or, imagine edge on dusty starbursts where the continuum may be completely obscured while Ly α escapes from extra-planar ionized gas (e.g. M 82).

High- z LAE selection methods are biased towards high EWs. Are current LAE samples representative in general of galaxies where Ly α photons are produced? Probably not. Total Ly α and UV luminosity densities for LAE samples at different z have been derived (e.g. Gronwall et al. 2007, Ouchi et al. 2008) from which (lower limits to) their star formation rate (SFR) can be derived. Comparing to UV selected LBG samples, LAEs make up 20 – 40% of the UV derived SFR density. This suggests that the relative escape fraction of Ly α , compared to UV, may be close to this value. However, the UV based SFR is an order of magnitude smaller than the total estimate, so the total average Ly α escape fraction would be on the order of a few percent. Hence, only a minor fraction of the galaxies where Ly α is created allows it to escape. In general though, comparing Ly α and UV based SFRs is tricky since they are sensitive to different age spans over which the star formation rate is likely not constant. Moreover, most estimates are based on derivations that assume steady-state star formation (e.g. Kennicutt 1998) which may not be relevant for LAEs.

The low Ly α escape fractions for local galaxies cannot be explained by standard reddening corrections. Is this result representative of high- z LAEs? Es-

escape fractions of a few percent seem to allow semi-analytic models to reproduce luminosity functions (Lacey this conference), but part of the audience seemed uncomfortable with such low f_{esc} for high- z sources. Again, observational techniques will favor galaxies with high escape fractions, meaning that current samples are biased.

Is the anti-correlated EWs of Ly α and H α found locally statistically significant? Does it apply at high- z ? Currently the answer to both these questions are unknown due to the lack of a statistical sample observed in both Ly α and H α (at any redshift). Establishing the Ly α vs. H α relation in different environments holds the clue to understanding the astrophysics of Ly α escape.

4 Outlook

Local studies suffer from small number of objects studied. Observations are expensive and currently restricted to one observatory, the HST. As long as it and the relevant instrumentation works, Ly α spectroscopy and imaging of local sources will be possible.

The number of local objects with both Ly α imaging, high resolution spectroscopy, and supplementary H α and H β data is very small.

To fully explain the radiative transfer of Ly α in galaxies, the imaging and spectroscopy should be supplemented with data of the neutral ISM column density and kinematics, at a similar spatial resolution. With current radio observatories, this is very challenging. One possibility to be explored is to use IFUs and optical lines like NaD.

High- z studies yield numerous LAEs, but most are too faint to allow detailed astrophysical investigations. Therefore, local studies will remain important, and at moderate redshift these approaches can potentially meet.

5 Acknowledgments

Thanks to Kim and the Local Organizing Committee for arranging such a nice conference! Thanks to the participants in this discussion section for making it interesting. Thanks to the conference attendees and fellow SOC members for interesting discussions. Thanks to Kim Nilsson and Matt Hayes for comments on this manuscript.

References

- Atek, H., Kunth, D., Hayes, M., Östlin, G., & Mas-Hesse, J.M., 2008, A&A 488, 491
- Charlot, S. & Fall, S.M., 1993, ApJ 378, 471
- Deharveng, J.M., Small, T., Barlow, T., et al., 2008, ApJ 680, 1072
- Giavalisco, M., Koratkar, A., & Calzetti, D., 1996, ApJ 466, 831
- Gronwall, C., Ciardullo, R., Hickey, T., et al., 2007, ApJ 667, 79
- Hayes, M., & Östlin, G., 2006 A&A 460, 681
- Hayes, M., Östlin, G., Atek, H., et al., 2007, MNRAS 382, 1465
- Hayes, M., Östlin, G., Mas-Hesse, J.M., & Kunth, D., 2009, arXiv 0803.1176
- Kennicutt, R., 1998, ARA&A 36, 189
- Kunth, D., Mas-Hesse, J.M., Terlevich, E., et al., 1998, A&A 334, 11
- Mas-Hesse, J.M., Kunth, D., Tenorio-Tagle, G., et al., 2003 ApJ, 598, 858
- Neufeld, D., 1991, ApJ 370, L85
- Ouchi, M., Shimasaku, K., Akiyama, M., et al., 2008, ApJS 176, 301
- Partridge, R.B., & Peebles P.J.E., 1967, ApJ 147, 868
- Shapley, A.E., Steidel, C.C., Pettini, M., & Adelberger K., 2003, ApJ 588, 65
- Verhamme, A., Schaerer, D., Atek, H., & Tapken, C., 2008, A&A 491, 89
- Östlin, G., Hayes, M., Kunth, D., et al., 2009, arXiv 0803.1174

Clustering of Lyman-Alpha Emitters Galaxies

Harold Francke

Departamento de Astronomía, Universidad de Chile, Casilla 36-D, Santiago, Chile

Abstract

Galaxy clustering properties have been studied for decades to constrain cosmological parameters and have today, with large datasets of high-redshift sources piling up, become a powerful tool to discriminate and characterize primeval galaxies. In the last years, several Lyman-Alpha Emitter (LAE) galaxy samples have been gathered, which are big, uniform and compact enough to allow clustering analysis. Here we present a summary of the discussion session on the clustering properties of LAEs at the “Understanding Lyman-alpha emitters” conference.

Key words: clustering, high-redshift, galaxies, Lyman-Alpha Emitters

1 Introduction

Clustering strength is one of the fundamental properties of a galaxy population, and a key quantity to include in any complete description of a sample. Galaxies are thought to form at density peaks, and thus to be biased tracers of the underlying matter field (Kaiser, 1984; Bardeen et al., 1986). In the current paradigm of hierarchical cosmology, where the structure formation and evolution is driven by the dynamics of dark matter, the effect of gravity reflects directly on the distribution of galaxies at the largest scales. The analysis of clustering can tell us the place of a given set of galaxies in the hierarchy of the large scale structure of the universe, by giving a measurement of the masses of the dark matter halos that host these galaxies. Furthermore, following the dynamics of these halos can help us in drawing an evolutionary picture between the different set of galaxies we observe in the distant and local universe. The advantage of this approach is that it gives information that is complementary to what is obtained from the light itself, i.e. from the analysis of the spectral energy distribution of the galaxies, or the morphological classification.

Measuring clustering properties requires the assembly of a homogeneous, spatially compact and numerous sample of objects, but also of a sample that

shows a small level of contamination. Obtaining samples of these galaxies large enough to allow clustering studies is only now becoming a reality and currently, results for Lyman Alpha Emitters (LAEs) are relatively scarce and prone to systematics. Ouchi et al. (2003) calculated the spatial correlation function of 87 sources at $z = 4.86$ in an area of 543 arcmin^2 of the Subaru Deep Field and found a fairly large correlation length, similar to LBGs at this redshift. Shimasaku et al. (2004) reported, in a follow-up work on the same field, that in a neighboring sample of 51 LAEs at $z = 4.79$ they found very weak clustering, and concluded that cosmic variance was a significant source of error in these surveys. Hayashino et al. (2004), imaging a 1088 arcmin^2 area around the SSA22a field previously studied by Steidel et al. (2000), found a significantly clustered population of 283 LAEs, something that is not a surprise, given the presence of a protocluster at $z = 3.09$ in the SSA22a subfield. They also detected 49 $\text{Ly}\alpha$ absorbers from their *decrement* in the narrow band flux with respect to the broadband flux. More recently, Kovač et al. (2007) were able to measure the spatial correlation function of a sample of 151 LAEs at $z = 4.5$ in the Large Area Lyman Alpha survey (LALA), covering an area of 1296 arcmin^2 . This result also shows LAEs with significant clustering strength, consistent with halos similar to Lyman-Break Galaxy halos, but with an occupation fraction of only 6 – 50%. In contrast, Gawiser et al. (2007), studying a sample of 162 LAEs in the ECDF-S field (992 arcmin^2) of the Multiwavelength Survey by Yale-Chile (MUSYC), found that at $z = 3.1$, these sources show a fairly low level of clustering, consistent with halos having a threshold mass of $4 \times 10^{10} M_{\odot}$. Following the growth of these low-mass halos in ΛCDM cosmology implied that these LAEs might be the progenitors of an important fraction of Milky-Way-sized galaxies.

2 Clustering measurements in LAE samples

The most popular measure of clustering strength is the two-point correlation function, both because of its simplicity and robustness. The angular autocorrelation function is defined as the excess probability of finding two galaxies separated by an angular distance θ .

$$\delta P_{12} = \Sigma^2 (1 + \omega(\theta_{12})) \delta\Omega_1 \delta\Omega_2 \quad (1)$$

where Σ is the mean density of data points and δP_{12} is the number of pairs between the area elements $\delta\Omega_1$ and $\delta\Omega_2$. The excess is defined relative to a uniform random Poisson distribution, for which $\omega(\theta)=0$. If object positions are correlated at scale r , then $\omega(\theta) > 0$, and if they are anti-correlated, i.e. they avoid each other at that scale, then $\omega(\theta) < 0$. To actually calculate this quantity from data, the most popular estimator used is the one proposed by

Landy & Szalay (1993):

$$\hat{\omega}_{LS}(\theta) = \frac{DD(\theta) - 2DR(\theta) + RR(\theta)}{RR(\theta)}. \quad (2)$$

where DD, DR and RR are the number of unique galaxy-galaxy, galaxy-random and random-random pairs separated by θ , normalized by the total number of pairs in each case, n is the number of galaxies in the data catalog and n_r is the number of points in the random catalog. The latter is supposed to describe the survey shape, in the sense that its distribution should be the result of observing a field of points with uniform, Poisson distribution over the same area, and in the same way the galaxy field was observed.

The effect of computing the clustering from a finite catalogue, with a mean density slightly different than the average in the universe, has long been recognized as a non-negligible bias that had to be accounted for. When Landy & Szalay calculated the expectation value and the variance of their estimator (2), they obtained:

$$\langle \hat{\omega}_{LS}(\theta) \rangle = \frac{\omega(\theta) - \omega_\Omega}{1 + \omega_\Omega} \approx \omega(\theta) - \omega_\Omega \quad (3)$$

$$\sigma_{LS}^2(\theta) = \frac{(1 + \langle \omega_{LS}(\theta) \rangle)^2}{(n(n-1)/2)RR(\theta)} \quad (4)$$

where ω_Ω is the so called “integral constraint factor”, calculated from:

$$\omega_\Omega = \frac{1}{\Omega^2} \int \int_{survey} \omega(\theta_{12}) d\Omega_1 d\Omega_2 = \int_0^{\theta_{MAX}} RR(\theta) \omega(\theta) d\theta \quad (5)$$

This appears in the calculation from Landy & Szalay as a normalization constant, but other authors derived this differently (Hamilton, 1993; Adelberger et al., 2005). The right hand side of this last equation comes directly from the definition of RR, and is used to numerically estimate this quantity from the number of RR counts. Ω is the field’s total solid angle. Typically, the linear approximation on the right hand side of equation 3 is the expression used to fit the measured autocorrelation function. Since ω_Ω depends on $\omega(\theta)$, the value for ω_Ω has to be consistent with the amount of clustering measured.

The expressions for the spatial correlation function are analogous to these, but of course require distance information on each of the galaxies. If good quality redshifts are available for a subset of the sample only, as usual, then the angular correlation function $\omega(\theta)$ has to be de-projected to obtain the spatial one, $\xi(r)$, from which physical quantities can be derived. If the time evolution

of the spatial autocorrelation function is negligible within the redshift range of the sample, as is in the case of a typical LAE selection, then the projection into $\omega(\theta)$ is given by:

$$\omega(\theta) = \int_0^\infty \int_0^\infty dr_1 dr_2 p(r_1) p(r_2) \xi \left(\sqrt{r_1^2 + r_2^2 - 2r_1 r_2 \cos \theta} \right) \quad (6)$$

where $p(r)$ is the co-moving radial distance distribution of the sample. The approximation made by Limber consists in assuming that the width of the functions p_1 and p_2 is much greater than the correlation length of ξ . This decouples both integrals and simplifies the computation (see Simon, 2007, for a derivation of this):

$$\omega(\theta) \approx \int_0^\infty d\bar{r} p(\bar{r})^2 \int_{-\infty}^\infty d\Delta r \xi \left(\sqrt{2\bar{r}^2(1 - \cos \theta) + \frac{\Delta r^2}{2}(1 + \cos \theta)} \right). \quad (7)$$

Simon (2007) showed that Limber’s approximation for the de-projection equation breaks down for surveys with narrow redshift distributions, such as in the case of LAEs, and fitting a single power law for $\omega(\theta)$ could bias the results. The difference between equations 6 and 7 is basically that Limber’s equation yields a power law ω for a power law ξ , while the non-approximated expression, given in equation 6, yields a broken power law ω for a power law ξ . If the slope of the spatial correlation function ξ is γ , then Limber’s equation yields the observed angular correlation function ω with a slope of $\gamma - 1$. The full, unapproximated expression gives this results only on small scales, but for angular separations bigger than some θ_{break} , the slope of ω becomes steeper, equal to γ . Notice that the Limber approximation has nothing to do with the “small angle” approximation used to simplify the trigonometric functions in the previous equations. Thus, for de-projecting LAE correlation functions, Limber’s simplifying assumption should be avoided.

To deduce physical properties from $\xi(r)$, one has two basic options: compare to cosmological numerical simulations, or to rely on analytical prescriptions such as those derived from the Press-Schechter (P-S) formalism (Press & Schechter, 1974). Modern simulations cover a wide range in halo masses and volumes comparable to many of the modern high-redshift surveys, enabling a direct comparison with the autocorrelation function of dark matter halos. Additionally, is also possible to constrain the descendants and ancestors of the halos hosting LAEs, from the merger trees associated to the simulation. On the other hand, the “excursion set” extensions to the original P-S formalism (Bond et al., 1991; Mo & White, 1996; Sheth et al., 2001) gives, in addition to a refinement to the P-S dark matter halo mass function, a relation between the mass of the halos and their clustering strength. The modernized version

of the mass function reads (Sheth et al., 2001):

$$n_h(M, z)dM = \frac{\bar{\rho}}{M} A \sqrt{\frac{2a}{\pi}} (1 + (a\nu^2)^{-q}) e^{-a\nu^2/2} \left| \frac{d\nu}{dM} \right| dM \quad (8)$$

where the variable $\nu(M, z) = \delta_c / \sqrt{D(z)\sigma^2(M)}$, the constants are $\delta_c = 1.68$, $a = 0.707$, $q = 0.3$, $A = 0.322$ and $\bar{\rho}$ is the mean density of the universe; $D(z)$ is the cosmological growth factor and $\sigma^2(M)$ is the density contrast variance inside spheres containing a mass M . The relation between the halo and dark matter correlation functions (the “bias factor”) is given by:

$$b(M, z) = \sqrt{\frac{\xi_{h,M}}{\xi_{dm}}} \\ = 1 + \frac{1}{\delta_c(z)} \left(a\nu^2 + b(a\nu^2)^{1-c} - \frac{(a\nu^2)^c / \sqrt{a}}{(a\nu^2)^c + b(1-c)(1-c/2)} \right) \quad (9)$$

with the additional constants $b = 0.5$ and $c = 0.6$; and with ξ_{dm} the correlation function of dark matter, and $\xi_{h,M}$ the correlation function of a halo of mass M . Naturally, this applies purely to dark matter halos. The connecting point between galaxies with their hosting halos is the halo occupation distribution (HOD) model. At scales larger than the size of the halo, the way galaxies are distributed inside the halo are not relevant, and the relevant quantities to compare to observations are the galaxy number density and the *effective* bias factor of the galaxy population:

$$n_g(z) = \int_0^\infty n_h(M, z) N_g(M) dM \quad (10)$$

$$b_{\text{eff}} = \frac{\int_0^\infty n_h(M, z) N_g(M) b(M, z) dM}{\int_0^\infty n_h(M, z) N_g(M) dM}, \quad (11)$$

where the function $N_g(M)$ describes the number of galaxies in each halo. The simplest possible model is one where N_g is zero below certain threshold mass M_{min} and one above it, i.e. one galaxy per halo for halos having a minimum mass. Another popular, slightly more complicated model would be to add a power law behaviour to this simple model, i.e. $N_g = (M/M_1)^\alpha$ for $M > M_{\text{min}}$ and 0 for $M < M_{\text{min}}$. Naturally, constraining more complex models require better statistics, especially at the smallest scales, which are the most sensitive to these additional details. But also, probing the smallest scales requires some assumptions about the way galaxies are distributed inside their halos.

3 Discussion Session

One concern raised at the discussion session was that although the majority of galaxy populations seem to follow the classical assumption that they trace the underlying dark matter field, in the case of LAEs this may not be true. LAEs are detected for their excess in $\text{Ly}\alpha$, a resonant line, which is affected by complicated physical processes: the amount of star formation, galaxy geometry and dynamics, interstellar and intergalactic medium opacities, etc. Several measurements of LAE clustering indicate that the occupation fraction of LAEs is low, near $\sim 5\%$ (Kovač et al., 2007; Gawiser et al., 2007). Hamana et al. (2004) fitted HOD models to the sample of LAEs in the Subaru Deep Field ($z=4.86$), and found that they could not reconcile the clustering strength they measured with the observed number density of LAEs. One reason for this discrepancy could be that LAEs do not really trace dark matter, but greater statistics are required to measure the correlation function at small scales with precision and pursue HOD models further. A question was also raised, whether this last measurement is representative of the bulk of LAE population at this redshift, given that there is evidence that this field might have unusual high clustering (Shimasaku et al., 2004). One suggestion made was that a relevant measurement would be to determine whether there is a dependence on HOD parameters with environment for local galaxies.

Just as in the case of continuum selected galaxies, where there is a clear correlation between galaxy brightness and clustering strength, it would be necessary to measure how the LAE clustering changes with $\text{Ly}\alpha$ flux and/or equivalent width (EW), given that these quantities are what determines the selection of an object. The future survey HETDEX will help in this direction since a huge number of LAE are going to be detected spectroscopically. Another interesting possibility lies within dim LBG samples, which are shown to overlap with LAE samples and for which a significant number of spectra have already been taken, although within a much broader redshift range, typical of broad-band selection.

Another concern raised was the size of the current LAE samples, allowing clustering measurements to be made, but is subject to a significant uncertainty due to cosmic variance, which in turn might be biasing some or all of the results quoted here. The small redshift range targeted by current narrow-band filter surveys makes it easier to measure even small amounts of spatial clustering, given the small dilution of the signal due to projection in the radial distance. This also means that for the same solid angle in the sky, the volume being sampled is much smaller, and therefore, obtaining a fair sample of the universe using narrow band selection is harder. From a semi-analytical galaxy model, Orsi et al. (2008) estimated the correlation function variance expected for several current surveys, and found the impact of cosmic variance

in these measurements is significant, and conclude that future surveys should be planned to cover much bigger volumes.

4 Conclusions

The most important conclusions from this discussion were:

- Bigger volumes, with bigger samples of LAEs are needed to reduce the problem of cosmic variance.
- The dependence of clustering strength on $\text{Ly}\alpha$ flux and equivalent width must be determined, since those are the quantities governing LAE selection.
- Models of galaxy formation would need to include a prediction for the clustering at small scales, the so called “1-halo” term in correlation functions. At these scales, the way LAEs populate their halos becomes important, and predictions will be needed in order to have a model comparison for the measured HOD parameters.

References

- Adelberger, K. L., Steidel, C. C., Pettini, M., et al., 2005, *ApJ*, 619, 697
Bardeen, J. M., Bond, J. R., Kaiser, N., & Szalay, A. S., 1986, *ApJ*, 304, 15
Bond, J. R., Cole, S., Efstathiou, G., & Kaiser, N., 1991, *ApJ*, 379, 440
Gawiser, E., Francke, H., Lai, K., et al., 2007, *ApJ*, 671, 278
Hamana, T., Ouchi, M., Shimasaku, K., Kayo, I., & Suto, Y., 2004, *MNRAS*, 347, 813
Hamilton, A. J. S., 1993, *ApJ*, 417, 19
Hayashino, T., Matsuda, Y., Tamura, H., et al., 2004, *AJ*, 128, 2073
Kaiser, N., 1984., *ApJ*, 284, L9
Kovač, K., Somerville, R. S., Rhoads, J. E., Malhotra, S., & Wang, J., 2007, *ApJ*, 668, 15
Landy, S. D., & Szalay, A. S., 1993, *ApJ*, 412, 64
Mo, H. J., & White, S. D. M., 1996, *MNRAS*, 282, 347
Orsi, A., Lacey, C. G., Baugh, C. M., & Infante, L., 2008, *MNRAS*, 391, 1589
Ouchi, M., Shimasaku, K., Furusawa, H., et al., 2003, *ApJ*, 582, 60
Press, W. H., & Schechter, P., 1974, *ApJ*, 187, 425
Sheth, R. K., Mo, H. J., & Tormen, G., 2001, *MNRAS*, 323, 1
Shimasaku, K., Hayashino, T., Matsuda, Y., et al., 2004, *ApJ*, 605, L93
Simon, P., 2007, *A&A*, 473, 711
Steidel, C. C., Adelberger, K. L., Shapley, et al., 2000, *ApJ*, 532, 170

Spectral Energy Distribution Fitting: Application to Ly α -Emitting Galaxies[★]

Eric Gawiser

Department of Physics and Astronomy, Rutgers University

Abstract

Spectral Energy Distribution (SED) fitting is a well-developed astrophysical tool that has recently been applied to high-redshift Ly α -emitting galaxies. If rest-frame ultraviolet through near-infrared photometry is available, it allows the simultaneous determination of the star formation history and dust extinction of a galaxy. Ly α -emitter SED fitting results from the literature find star formation rates $\sim 3\text{M}_\odot \text{ yr}^{-1}$, stellar masses $\sim 10^9\text{M}_\odot$ for the general population but $\sim 10^{10}\text{M}_\odot$ for the subset detected by IRAC, and very low dust extinction, $A_V \leq 0.3$, although a couple of outlying analyses prefer significantly more dust and higher intrinsic star formation rates. A checklist of 14 critical choices that must be made when performing SED fitting is discussed.

Key words: galaxy formation, star formation, stellar populations, starburst galaxies, protogalaxies

PACS: 98.62.Ai, 98.62.Lv, 98.58.Hf, 98.54.Ep, 98.54.Kt

1 Spectral Energy Distribution Fitting

Although it is not widely recognized, Spectral Energy Distribution (SED) fitting and photometric redshift determination are identical. Both use the likelihood function $L(z, T)$ that a galaxy's observed SED was generated by template type T at redshift z . This is typically generated from

$$L(z, T) = \frac{\exp(-\chi^2/2)}{(2\pi)^{N/2} \prod_i \sigma_i}, \quad \text{where} \quad \chi^2 = \sum_i (p_i - o_i)^2 / \sigma_i^2, \quad (1)$$

[★] Based on a presentation and discussion at “Understanding Lyman-alpha Emitters”, MPIA, Heidelberg, Oct. 6-10, 2008

Email address: `gawiser@physics.rutgers.edu` (Eric Gawiser).

i indexes the N photometry bands, p are template predictions in these bands, o are observed fluxes and σ are observational errors. A best-fit normalization factor for each template/object combination can be solved for analytically to simplify optimization.

When only a photometric redshift is desired, one marginalizes or optimizes over the nuisance parameter T , and it usually suffices to use a limited set of templates. SED fitting typically involves a large set of templates at fixed redshift, corresponding to a delta-function prior in z . This is justified when a spectroscopic redshift is available but is a dubious practice otherwise. A common practice is to determine photometric redshifts with a limited template set, fix the redshift at the best fit, and then perform SED fitting with a wide range of templates. This is computationally convenient but statistically inconsistent, is guaranteed to underestimate the uncertainties, and runs the risk of biasing the results significantly.

Nonetheless, SED fitting is a robust, well-developed method at low redshift, where spectroscopic redshifts are typically available (see Kannappan and Gawiser, 2007 and references therein for discussions of applications and caveats). Ly α -Emitting (LAE) galaxies are well-suited to SED fitting because the narrow-band selection finds galaxies in a narrow enough redshift range that a fixed redshift can be assumed when fitting broad-band photometry. However, the signal-to-noise (S/N) available for photometry of these dim, high-redshift galaxies is considerably lower than for other galaxy types to which SED fitting has been applied. Hence we need to select SED methods that are appropriate for low S/N and to avoid over-fitting. Novel methods may be required to handle the unusual characteristics of these galaxies, in particular the guarantee from high equivalent-width emission-line selection that a starburst is occurring at the time of observation, the corresponding guarantee that other nebular emission lines are strong, and the opportunity to utilize narrow-band photometry as part of the SED.

Despite the low S/N available for LAEs, SED fitting has been claimed to allow the determination of star formation rate (SFR), stellar mass, stellar age, characteristic timescale for star formation (τ), dust extinction, and a new q parameter describing radiative transfer effects on Ly α photons (e.g., Finkelstein et al., 2007). When a starburst is occurring, the burst population is expected to dominate the rest-ultraviolet continuum. In the unusual case that dust extinction is negligible, the SFR is proportional to the rest-UV flux (Kennicutt, 1998) and the rest-UV slope depends on the age of the starburst and the shape of the initial mass function. In most galaxies, dust is too abundant for this interpretation to be meaningful, but in LAEs the selection method guarantees minimal dust extinction (see Fig. 14 of Gronwall et al., 2007). If dust extinction is not too high, the rest-NIR luminosity density is nearly directly proportional to the stellar mass, with some dependence on the age of

the stellar population traced by rest-optical color since older main-sequence stars have a higher mass-to-light ratio (Bell et al., 2003; Portinari et al., 2004).

2 Results for Ly α -emitting Galaxies

Table 1 includes all reported results for emission-line-selected LAEs as of October, 2008. This compilation does not include objects initially selected in the continuum that turned out to show strong Ly α emission (Pentericci et al., 2009); these should be referred to as, e.g., Ly α -emitting Lyman break galaxies, rather than LAEs. All observations find similar rest-UV flux densities, hence analyses with large inferred dust extinction also report very large intrinsic SFR. Significant scatter exists in the age results, partially due to wide variation in model assumptions between constant SFR, τ and instantaneous burst models. The only robust determinations are of star formation rates $\sim 3M_{\odot} \text{ yr}^{-1}$, stellar masses $\sim 10^9 M_{\odot}$ for the general population but $\sim 10^{10} M_{\odot}$ for the subset detected by IRAC, and of very low dust extinction, $A_V \leq 0.3$, although a couple of outlying analyses prefer significantly more dust and correspondingly higher intrinsic star formation rates.

Discussion about the current results included concerns that systematic effects due to different analysis methods on these parameters can be serious. To estimate the severity of this, we agreed to trade SEDs to be analyzed by other groups using their methods to see how much difference is produced in the best-fit parameters and their reported uncertainties. Significant effort should be invested in developing a more consistent fitting method than the various ones used to obtain the current literature results. Determining evolution of LAE results with redshift or comparisons of LAEs and LBGs requires applying a common analysis method, as in the posters by S. Yuma and K. Ohta at this meeting.

3 Discussion: 14 SED Fitting Choices

In this section we discuss 14 choices necessary for any modeler to make when preparing and fit of observed galaxy SEDs.

1. Stellar population models: One typically chooses a set of stellar population models from BC03 (Bruzual and Charlot 2003), M05 (Maraston 2005), or the unpublished CB08 (Charlot-Bruzual 2008) models. The M05 and CB08 models include the empirically-determined contribution of thermally pulsating asymptotic giant branch (TP-AGB) stars, which makes a major difference in rest-NIR photometry at intermediate ages. So BC03 should be avoided,

Table 1

Results from F08b (Finkelstein et al., 2009), G07 (Gawiser et al., 2007), L07 (Lai et al., 2007), L08 (Lai et al., 2008), N07 (Nilsson et al., 2007), and P07 (Pirzkal et al., 2007). NI (I) means that analysis was restricted to LAEs lacking (having) IRAC detections. Analyses by G07, L08 and N07 are of stacked populations, whereas other results show the average and scatter amongst results for individual LAEs, with all error bars corresponding to the 68% confidence level. Where two-population fitting was used (G07, F08b, P07), age and τ refer to the younger population and young fraction is the fraction of the total stellar mass given in the 5th column that resides in the young population; if single-population fitting was used, young fraction is set to 1. If a constant SFR (instantaneous burst) was assumed, τ is set to ∞ (0). The F08b results for radiative transfer of Ly α photons yield $q = 1.0^{+2.8}_{-0.4}$.

Ref	z	SFR	A_V	Stellar mass	age	τ	young
		[$M_{\odot}\text{yr}^{-1}$]	[mag]	[$10^9 M_{\odot}$]	[Myr]	[Myr]	fraction
G07_NI	3.1	2 ± 1	$0.0^{+0.1}_{-0.0}$	$1.0^{+0.6}_{-0.4}$	20^{+30}_{-10}	750 ± 250	$0.2^{+0.3}_{-0.1}$
L08_NI	3.1	2 ± 1	$0.0^{+0.3}_{-0.0}$	$0.3^{+0.4}_{-0.2}$	160^{+140}_{-110}	∞	1
L08_I	3.1	6 ± 1	$0.0^{+0.3}_{-0.0}$	9 ± 3	1600 ± 400	∞	1
N07	3.15	$0.7^{+0.5}_{-0.3}$	$0.3^{+0.1}_{-0.2}$	$0.5^{+0.4}_{-0.3}$	850^{+130}_{-420}	∞	1
F08b	4.5	140^{+170}_{-110}	0.5 ± 0.2	15^{+35}_{-14}	13^{+500}_{-7}	0	0.4 ± 0.4
P07	~ 5	8 ± 1	0.1 ± 0.1	$0.2^{+0.3}_{-0.1}$	4^{+4}_{-3}	0	$0.2^{+0.4}_{-0.2}$
L07_I	5.7	400^{+600}_{-370}	0.7 ± 0.4	17 ± 13	500 ± 400	∞	1

although the difference is largest at solar metallicity and less severe for the lower metallicities likely for LAEs. The discussion pointed out that Starburst99 (Leitherer et al., 1999; Vázquez and Leitherer, 2005) models include nebular emission, which the above models do not. They have been updated to include TP-AGB stars (Vázquez and Leitherer, 2005) and should properly handle populations as young as 1 Myr, whereas the above models should not be trusted for young starbursts due to the lack of nebular continuum and emission lines. However, the effects of metallicity and ionization parameter, both of which are unknown for LAEs, become important when using these models.

2. Star formation history: In hierarchical cosmology, we expect galaxies to have complex star formation histories that combine a series of starbursts with quiescent star formation, with the average SFR increasing versus time during the early stages of galaxy formation before the supply of neutral gas becomes exhausted. In practice, SED-fitting approximates this using a smooth history, $SFR(t) = SFR(t_0) \exp(-(t - t_0)/\tau)$, where the SFR is assumed to be zero before t_0 and the stellar age at the time of observation is $t_{obs} - t_0$. A Constant Star Formation rate (CSF) corresponds to $\tau \rightarrow \infty$ and a Simple Stellar Population (SSP) corresponds to a delta-function SFR at t_0 (approx-

imated by $\tau \rightarrow 0$). Negative values of τ should be included in fits as they correspond to an exponentially increasing SFR which is what would result from a constant *specific* star formation rate. Finlator et al. (2007) compared these smooth star formation histories with realistic bursty ones from cosmological hydrodynamic simulations and found that both produced acceptable fits to high-redshift observations.

3. Minimum age: The maximum age that a stellar population should be allowed to have is the age of the universe at the time of observation. This is mildly unrealistic, as a large SFR at the instant of the Big Bang makes little sense, but the observational consequences at $z < 6$ of beginning star formation at $z = \infty$ versus e.g., $z = 15$ are small given the short time difference. The minimum age is a subtler question. Following the discussion above, one should use Starburst99 (or the equivalent) for modeling any population younger than ~ 10 Myr while varying the input metallicity and ionization parameter.

4. Initial mass function (IMF): Although it is often stated that the IMF appears universal, a top-heavy IMF at high-redshift has recently been claimed (van Dokkum, 2008; Davé, 2008) and has been used to model LAEs (Le Delliou et al., 2006). Even different versions of the “universal” local IMF make a factor of two difference in stellar mass. This difference can be corrected for when comparing results as long as all papers report their assumed IMF. During the discussion it was suggested to use a Salpeter IMF between 100 and 0.01 solar masses as a common standard to enable comparison of results.

5. Metallicity range: Since the metallicities of LAEs have yet to be measured, a conservative approach is to allow this parameter to vary between $0.01 Z_{\odot}$ and Z_{\odot} . In theory, SED fitting can be used to fit the metallicity, but the effect is minor and is degenerate with other parameters, so it is best to consider this as a systematic uncertainty. The discussion pointed out that assuming a single metallicity causes an underestimate in the age uncertainty due to age-metallicity degeneracy in SED shape.

6. Dust law: The Calzetti et al. (2000) dust law gives the dust extinction as a function of wavelength, parametrized by $E(B-V) = 0.3 A_V$. Calibrated to local starburst galaxies, this is the dust law typically used for high-redshift SED fitting. However, we do not know if the dust law evolves with redshift, and given local variations we should consider this a significant uncertainty. It would therefore be useful to vary the dust law from Calzetti to SMC to Milky Way dust and to report the amplitude of uncertainties caused in other SED fitting parameters. The idea of removing dust from the fit was discussed; while defensible for LAEs where an absence of dust could be assumed, this could make it more difficult to compare results with other galaxy types where dust is clearly present.

7. IGM absorption: A model for absorption by the intergalactic medium (IGM) must be applied to template spectra. Most commonly this follows Madau (1995) but during the discussion updated analyses by Songaila (2004) and Faucher-Giguère et al. (2008) were recommended. These references provide a method for modeling IGM absorption of continuum emission, but the prescription that should be applied to Ly α emission is unclear. Naively, all photons blue-wards of 1215.67Å rest-frame suffer IGM absorption, but the treatment in the literature varies from assuming no IGM effect on Ly α to assuming that fully half the Ly α photons have been absorbed by the IGM. Radiative transfer effects from resonant scattering and galactic winds are too complex to yield an obvious recipe, as the simulations of Verhamme et al. (2006) have shown. This provides a motivation for removing Ly α emission from the SED fit by ignoring the narrow-band photometry, although more advanced options are described below.

8. Number of stellar populations: Fitting a simple stellar population to an LAE is not a good approach if one is interested in determining age and total stellar mass. The presence of a starburst guarantees a young age and a low implied stellar mass for an SSP. Even CSF and τ models are poorly suited for modeling a star formation history that is likely to have made a rapid upward jump at the beginning of the starburst (possibly due to a galaxy merger). Allowing exponentially increasing SFR through negative values of τ will help somewhat. However, we need to utilize multiple-population SED models, as done by Pirzkal et al. (2007) and Gawiser et al. (2007) to reveal any underlying population of old stars whose star formation history does not smoothly tie onto the active starburst.

However, as noted above, the low S/N available with LAE SEDs makes it important to avoid fitting too many parameters. Even an SED with 13 bands (*UBVRIZJHK*[3.6][4.5][5.8][8.0]) can lead to degeneracies when fitting a dozen parameters plus the overall normalization. Each stellar population comes with 4 degrees of freedom: instantaneous SFR, age, τ , and A_V (stellar mass is determined by the first three). So we clearly cannot afford to fit more than two populations, and there are benefits to reducing the degrees of freedom by simplifying the populations e.g., by assuming a model at the age of the universe for the old population. Gawiser et al. (2007) assumed that both populations see the same dust extinction; although this assumption is probably not true in general, it is very difficult to determine the dust reddening for an older population detected in only a couple IRAC bands where it dominates the photometry. It may make the most sense to combine a young model from Starburst99 with an old model from e.g. M05.

9. Individual SEDs or stacked? Low S/N makes it difficult to obtain robust results from SED fitting of individual LAEs, although several papers have chosen this approach. An alternative is to average (“stack”) the pho-

tometry of an entire sample of LAEs. The latter approach achieves greater S/N at the cost of revealing “average” SED parameters for the entire LAE population rather than individual objects. Finkelstein et al. (2009) compared these methods and demonstrated that the average of individual LAE SED parameters was somewhat similar to the SED parameters fit to the average LAE SED, although a more detailed investigation is needed to be able to properly compare stacked and individual SED fit parameters. The discussion pointed out that if an analysis splits a population of objects into subsets based upon, e.g., $[3.6]\mu\text{m}$ flux, one should perform simulations to identify and subtract Malmquist-type biases caused by noise in the resulting SED parameters (noise causes the $[3.6]\mu\text{m}$ flux to be overestimated for the brighter stack and underestimated for the dimmer stack).

10. Include nebular emission lines? An important decision in SED fitting is whether to include nebular emission lines in the template spectra. As Zackrisson et al. (2008) have pointed out, these nebular emission lines can make a significant difference in SED fitting and photometric redshifts but are usually neglected. For very young populations at $4 < z < 5$, $\text{H}\alpha$ can make a significant contribution to the $[3.6]\mu\text{m}$ photometry. BC03 models report the number of ionizing photons, which can be turned into $\text{Ly}\alpha$ and Balmer series luminosities assuming Case B recombination. Starburst99 does this automatically and includes the critical [O II] and [O III] emission lines.

11. Treatment of narrow-band photometry: Since spectral templates typically do not include emission lines and $\text{Ly}\alpha$ is particularly complicated, the most common approach has been to ignore the narrow-band photometry of LAEs. Sometimes the inferred $\text{Ly}\alpha$ flux is used to subtract the emission-line contribution from overlapping broad-band photometry. This is sensible, although the uncertainty in this correction should be propagated into the photometric uncertainties on the broadband fluxes. One caveat when using photometry from a narrow-band filter with a rounded (rather than top-hat) response curve is to avoid assuming that the LAEs are all at the redshift corresponding to the peak filter transmission, as this will systematically underestimate the objects’ true $\text{Ly}\alpha$ fluxes. Ideally the redshift should be varied, and the filter transmission can at least be represented by a more typical value (see Gronwall et al., 2007).

A well-motivated attempt has recently been made by Finkelstein et al. (2007, 2008, 2009) to incorporate $\text{Ly}\alpha$ emission in the spectral templates to be compared with the full LAE SEDs including narrow-band photometry. These authors introduced a new SED parameter, q , where $q = 1$ implies trivial radiative transfer, $q < 1$ implies the expected preferential extinction of $\text{Ly}\alpha$ photons, and $q > 1$ implies that $\text{Ly}\alpha$ photons are enhanced versus continuum photons (either by anisotropic radiative transfer or possible clumpy dust as described by Neufeld, 1991). The combination of SFR, stellar age, and dust is sufficient

to predict the Ly α flux when $q = 1$, and comparison with the continuum-subtracted narrow-band flux density determines q . The discussion appeared to produce agreement that in this sense q is independent of the broad-band SED fit and could be determined subsequently to simplify computation.

12. Treatment of photometric uncertainties: When population-averaged fluxes are being used, a bootstrap analysis can be performed to include sample variance in the photometric uncertainties; this usually dominates the formal uncertainty in the average flux so is important to include. The discussion illuminated concerns about systematic errors in photometry, due primarily to the difficulty of performing aperture photometry in the IRAC bands given the much larger PSF and significant source confusion.

Some statistically dubious habits have crept into the LAE SED fitting literature with authors excluding “non-detections” from the fits or only penalizing the χ^2 when a template flux exceeds a 3σ upper limit. This alters the χ^2 statistic to *no longer follow a χ^2 distribution*, making interpretation difficult. Moreover, this modification is entirely unnecessary when SED fitting is done in flux (magnitudes should be avoided at all costs given the asymmetry of errors at low S/N). For low S/N data, noise fluctuations can cause negative fluxes, and these fluctuations are properly handled by feeding χ^2 the observed fluxes and their formal photometric uncertainties. The related practice of only plotting photometry for bands with formal 3σ detections is less dangerous but equally hard to justify.

13. Method for determining best-fit model: Producing a likelihood for a single template is straightforward, but over a large parameter space the brute-force approach of determining the likelihood for every possible template can be very computationally intensive. Some authors are simplifying this using Markov-Chain Monte Carlo (MCMC), for which public routines exist. MCMC tries to avoid getting stuck in local minima, but extensive testing is still recommended to be sure that the global optimum is being found successfully. Another decision to be made is frequentist versus Bayesian interpretation of this likelihood (see Lupton, 1993). A frequentist analysis will simply call the template with maximum likelihood the best fit, whereas a Bayesian analysis will choose prior probabilities on all of the parameters and marginalize over these to report the best fit parameter set.

14. Method for determining parameter uncertainties: The final choice to be made is how to determine the uncertainties in the best-fit SED parameters. The most common method is to use $\Delta\chi^2$ where the χ^2 value is allowed to increase by the right amount to represent the 95% confidence level for the given number of degrees of freedom, n_{dof} . However, frequentist analysis actually recommends ruling out only those parameter values for which no template is a good fit to the data (despite considering all possible values

of other parameters) using absolute values of χ^2 rather than $\Delta\chi^2$. Unless the error bars are underestimated, this is quite conservative. Many astrophysicists instead use the Bayesian approach, where a “credible region” on a given parameter is determined by projecting the likelihood function onto that single dimension, marginalizing over all other parameters, and keeping the parameter range that contains e.g. 95% of the posterior probability. To fully grasp parameter dependencies and correlations, the full dimensional parameter space must be studied. Monte Carlo simulations can also be performed by varying the observed photometry within its reported uncertainties and determining the range of best-fit parameters. This is a reasonable approximation but is not statistically self-consistent. For example, a particular model might be an acceptable fit to all of these simulations but never end up as the best fit, so the parameter range of “best fits” can underestimate the true uncertainties. MCMC codes produce uncertainties along with their best fits.

Discussion ensued over how to determine the number of degrees of freedom. It depends on whether a single model or an entire parameter space is being evaluated. For a model, $n_{\text{dof}} = n_{\text{data}} - n_{\text{nuisance}}$, where the final term is the number of nuisance parameters being fit such as the overall normalization. For a parameter space, $n_{\text{dof}} = n_{\text{data}} - n_{\text{parameter}}$, which essentially corresponds to treating all parameters as nuisance parameters to see if *any* model in this entire space is an acceptable fit to the data.

4 Acknowledgments

I thank the conference organizers for a well-organized, extremely pedagogically useful meeting, and participants in the SED fitting discussion for contributing ideas recounted here. Len Cowie deserves special mention for making numerous valuable suggestions. I wish to thank Kim Nilsson for creating the figures used for my review discussion at the meeting, Suraphong Yuma for providing the summary of LAE SED fitting results from his poster at the meeting and Steve Finkelstein for sending the error bars on his published SED fitting results shown in the table. I acknowledge financial support for LAE SED research from Spitzer Space Telescope archival programs AR-40823 and AR-50805.

References

- Bell, E.F., McIntosh, D.H., Katz, N., & Weinberg, M.D., 2003, ApJS, 149, 289
- Bruzual, G., & Charlot, S., 2003, MNRAS, 344, 1000
- Calzetti, D., Armus, L., Bohlin, R.C., et al., 2000, AJ, 533, 682
- Davé, R., 2008, MNRAS, 385, 147

- Faucher-Giguère, C.-A., Prochaska, J.X., Lidz, A., Hernquist, L., & Zaldarriaga, M., 2008, *ApJ*, 681, 831
- Finkelstein, S.L., Rhoads, J.E., Malhotra, S., Pirzkal, N., & Wang, J., 2007, *ApJ*, 660, 1023
- Finkelstein, S.L., Rhoads, J.E., Malhotra, S., Grogan, N., & Wang, J., 2008, *ApJ*, 678, 655
- Finkelstein, S.L., Rhoads, J.E., Malhotra, S., & Grogan, N., 2009, *ApJ*, 691, 465
- Finlator, K., Davé, R., & Oppenheimer, B.D., 2007, *MNRAS*, 376, 1861
- Gawiser, E., Francke, H., Lai, K., et al., 2007, *ApJ*, 671, 278
- Gronwall, C., Ciardullo, R., Hickey, T., et al., 2007, *ApJ*, 667, 79
- Kannappan, S.J., & Gawiser, E., 2007, *ApJ*, 657, L5
- Kennicutt, Jr., R.C., 1998, *ARAA*, 36, 189
- Lai, K., Huang, J.-S., Fazio, G., et al., 2007, *ApJ*, 655, 704
- Lai, K., Huang, J.-S., Fazio, G., et al., 2008, *ApJ*, 674, 70
- Le Delliou, M., Lacey, C.G., Baugh, C.M., & Morris, S.L., 2006, *MNRAS*, 365, 712
- Leitherer, C., Schaerer, D., Goldader, J.D., et al., 1999, *ApJS*, 123, 3
- Lupton, R., 1993, *Statistics in Theory and Practice*, Princeton University Press.
- Madau, P., 1995, *ApJ*, 441, 18
- Maraston, C., 2005, *MNRAS*, 362, 799
- Neufeld, D.A., 1991, *ApJ*, 370, L85
- Nilsson, K.K., Møller, P., Möller, O., et al., 2007, *A&A*, 471, 71
- Pentericci, L., Grazian, A., Fontana, A., et al., 2009, *A&A*, 494, 553
- Pirzkal, N., Malhotra, S., Rhoads, J.E., & Xu, C., 2007, *ApJ*, 667, 49
- Portinari, L., Sommer-Larsen, J., & Tantalo, R., 2004, *MNRAS*, 347, 691
- Songaila, A., 2004, *AJ*, 127, 2598
- van Dokkum, P.G., 2008, *ApJ*, 674, 29
- Vázquez, G.A., & Leitherer, C., 2005, *ApJ*, 621, 695
- Verhamme, A., Schaerer, D., & Maselli, A., 2006, *A&A*, 460, 397
- Zackrisson, E., Bergvall, N., & Leitet, E., 2008, *ApJ*, 676, L9

Lyman α Blobs: Discussions in Heidelberg

Toru Yamada

Astronomical Institute, Tohoku University, Aoba-ku, Sendai 980-8578, Japan

Abstract

Ly α Blobs (LAB), large, extended Ly α emitters, are enigmatic objects that call on much attention in the field of galaxy formation and evolution. So far, discovery of more than twenty giant (> 60 kpc) LABs have been reported and new searches are on-going. Many of the groups who study LABs attended the workshop in Heidelberg, “Understanding Ly α Emitters”, 2008 Oct 6-10. We had useful discussions on the various important aspects of LABs including the search or detection methods, origins of the extended Ly α emission, and their physical properties.

Key words: galaxy formation, galaxy evolution

1 Introduction

In this discussion, we reviewed the current knowledge about Lyman α Blobs (LABs), or extended Ly α haloes at high redshift, mainly at $z \sim 2 - 4$.

Since their discovery, enigmatic LABs have called much attention in the field of galaxy formation, since extended Ly α emission should be observed at various stages during the major formation epoch of galaxies. First, they should be observed when the gas heated by virial shock in collapsed primordial dark-matter haloes are cooled by radiating Ly α emission. The expected properties were studied (Haiman et al. 2000; Fardal et al. 2001) and extended Ly α emission of these ‘cooling collapse’ objects were found to be observable. Secondly, galaxies experiencing major star formation, and UV radiation from the massive stars can ionize the surrounding HI gas. Since the formation of massive galaxies and super-massive black holes are closely and maybe causally connected, ionizing radiation from AGN may also contribute. Thirdly, supernova explosions or AGN feedback may heat the gas and cause a galactic super-wind. Extended Ly α emission is then also expected from the gas shock-ionized or excited by the galactic super-wind.

We have at least two clear motivations to search for and study LABs. While the star-forming galaxies at high redshift are generally compact and show significant negative size evolution (Ferguson et al. 2004), *extended* Ly α emission may indicate the presence of other physical processes than simple photoionization, such as cooling collapse or galactic super-winds. Even if the Ly α emission is simply due to the photoionization, their size may be scaled with mass of the galaxies. With LABs, we may study early stages of massive galaxy formation.

In the discussion, we focused on ‘radio-quiet’ Ly α haloes. Extended Ly α haloes at high redshift were first observed around powerful radio galaxies and radio-loud quasars. However, Ly α haloes around luminous radio-loud objects are likely to be powered by or closely related to their radio jet activities. Christensen et al. (2006) compared the Ly α haloes of radio-loud and radio-quiet quasars and found that luminosities and sizes of the Ly α halos of radio-loud quasars are much more luminous and larger than those of powerful radio-quiet quasars. Ly α emission of radio-loud objects are often elongated and show alignment to the radio axis. While it is true that the extended Ly α haloes of at least some powerful radio galaxies may not be explained fully by the radio-jet activity and they indeed show signs of massive galaxy formation (e.g., N. Hatch, in this workshop), the origin of the very luminous haloes must be more causally related to their radio-jet activities.

So far, more than 20 giant Ly α Blobs (sometimes called Ly α haloes) larger than ~ 60 kpc, and more than 100 LABs larger than ~ 30 kpc have been detected and reported by October 2008. The summary of the authors of the known LABs larger than ~ 20 kpc was presented (Keel et al. 1999; Steidel et al. 2000; Matsuda et al. 2004; Palunas et al. 2004; Dey et al. 2004; Nilsson et al. 2006; Smith & Jarvis 2007; Saito et al. 2008; Ivison et al. 1998; Greve et al. 2007; Ouchi et al. 2008; and Yang et al., Matsuda et al., Prescott et al., Smith et al. in this workshop).

2 Search, Detection, and Identification

Since the discovery of the first LABs (Keel et al. 1999; Steidel et al. 2000), the definition of an LAB has been rather vague. They are *extended* objects in Ly α emission with rather blobby structure. But what does “extended” mean? In many cases, authors just refer the size of LABs by the dimension above some surface brightness threshold which is not even clearly given in some cases. Should we agree on a homogeneous way to define LABs? It is true that we cannot compare the LABs defined in different manner in their statistical properties such as number densities. On the other hand, the surface brightness profiles of LABs in their Ly α emission are not well characterized as a sample.

It is useful to note the difference in Ly α Emitters (LAE) and LABs. When we construct a sample of LAEs, we usually first detect sources above some deep surface brightness threshold and then do the aperture photometry at the peak or weighted center on the narrow-band images. The aperture size in these LAE searches is typically $2 - 3 \times$ FWHM of the seeing in order to get maximum S/N ratio to the background sky noise. Certainly this procedure may miss extended low-surface brightness sources. Thus an optimized detection method for LABs is needed as e.g. described above. Furthermore, one should take special care in the sky subtraction procedure. In the search for LABs, the local sky emission should be subtracted with sufficiently larger scale than the objects to be found. This may differ from the optimized procedure to detect the faintest LAEs. On the other hand, peaks in Ly α emission in LABs may be 'misidentified' as the isolated LAEs. Their source position are often displaced from the peaks of the continuum sources associated to the LABs.

There are various methods to search for LABs. There are surveys with shallow-depth and large area which are optimized to the most luminous LABs (Yang et al., this workshop) and deep moderate-area surveys (e.g., Matsuda et al. this workshop). For the luminous large objects, one may use intermediate-band filters (Saito et al. 2006) or even broad-band filters (e.g., Prescott et al., in this workshop). Compared to the search using narrow-band filters, these methods can search much larger volume and redshift range. New samples of giant luminous LABs have been detected by the method. A set of intermediate-band filters can cover a large continuous redshift range and thus very large volume.

There are a few different ways to define extended Ly α Emission, i.e., *i*) extension above the threshold surface brightness, *ii*) extension in their half-light radius, and/or *iii*) extension compared to their UV continuum. Among them, definition *iii*) may be the most uncertain for LABs as the Ly α emission is usually more extended than UV emission for most of the LAEs including even the compact objects. As mentioned above, since we have not succeeded to characterize the Ly α light profiles of LABs, the simple definition by their isophotal area or size may be useful for the moment. We should then change to using a more firm definition to classify and compare samples of LABs.

Matsuda et al. (2004) conducted the first systematic search for LABs. They adopted a surface brightness threshold of 2×10^{-18} erg s $^{-1}$ cm $^{-2}$, both for the source detection and identification of LABs. They then applied the criteria, EW_{obs} (isophotal) > 80 Å, isophotal area larger than 16 arcsec 2 (900 kpc 2 at $z = 3.1$), and then selected sources with more than 7σ in the isophotal photometry and with isophotal area larger than 2 times the PSF with the same average surface brightness. They applied the same criteria in their new extended search for LABs over 2 deg 2 . The average surface brightness reaches 4×10^{-18} erg s $^{-1}$ cm $^{-2}$. While the isophotal selection of LABs has a disad-

vantage that it depends on redshift and observation depth, it is probably the most suitable way in this discovery phase as one can search the most extended Ly α emission in a set of observations. With a sample of more than 100 LABs with sizes larger than 900 kpc², or $d \sim 30$ kpc, we can now investigate the light profiles of LABs and maybe find a good way to characterize their size independent of the redshift and image depth in the near future.

Relationships between LABs and LAEs or other high- z objects, such as Lyman Break Galaxies, Distant Red Galaxies, and Sub-mm Galaxies were also discussed. For the case of the LABs larger than ~ 30 kpc in Matsuda et al. (2004), LBGs (alone) are associated with $\sim 60\%$ of the LABs. For the case of the giant LABs, multiple objects such as LBGs, DRGs, and other objects at the consistent redshift are associated to the same LAB. For one blob (LAB18 in Matsuda et al. 2004), an extremely red object is observed at the center of the diffuse but very extended Ly α emission. It was also reported that LBGs and compact LAEs have very diffuse extended Ly α halos. In the stacked image, they show Ly α haloes larger than ~ 40 kpc. They were not detected as LABs as their sizes are much smaller at the detection threshold.

3 Origins of the Extended Ly α Emission

What powers the extended Ly α emission of LABs? We discussed three distinctive cases, namely, *i*) cooling collapse, *ii*) galactic super-wind, and *iii*) photo-ionization by massive stars or AGN, sometimes possibly hidden by dust extinction.

What are the signatures of cooling collapse? Very large equivalent widths (EW) may be one signature. In such objects, star-formation occurs only partially, maybe at the densest clump or the center of the gravitational potential. In extreme cases, only the extended Ly α emission is seen and nothing in any other wavelength. Nilsson et al. (2006) reported a candidate of such a very interesting source at $z = 3.16$ in GOODS-S. We have to be careful, however, to confirm that such objects are purely Ly α emitters by checking the various possibilities including the ionization by hidden AGN. For the case of Nilsson's object, no evidence of the associated continuum object has been reported so far. Another signature of the cooling collapse objects is the relatively flat surface-brightness profile predicted in Dijkstra et al. (2006). Nilsson et al. (2006) and Smith and Jarvis (2007) reported such flat profiles for their LABs at $z = 3.16$ and $z = 2.83$. A red, sharp cut-off in the Ly α line profile may be a signature of cooling collapse. Smith and Jarvis (2007) claimed to see such a feature in their LAB at $z = 2.83$. Diffuse HeII emission as an indicator of very hot gas ($T \sim 10^5$ K) may be expected among the objects in this category (Yang et al. 2006).

Next, what are the signatures of the galactic super-wind? Large velocity widths of $\sim 1000 - 2000 \text{ km s}^{-1}$ are observed in many LABs at $z = 2 - 3$ (Steidel et al. 2000; Ohyama et al. 2003; Dey et al. 2005; Wilman et al. 2005; and Matsuda et al. 2006). Wilman et al. (2005) show the existence of large-scale homogeneously-expanded HI gas in the Ly α profile of the SSA22-LAB2 at $z = 3.1$. Diffuse metal emission lines may be potential evidences of the galactic super-wind but detections of such diffuse extended emission have not been reported so far. Another possible evidence of the super-wind is the “shell-like” structure which resembles the super bubbles seen in local galaxies. Matsuda et al. (2004) reported shell-like structures in the deep narrow-band image of the SSA22-LAB1 and Mori and Umemura (2006) showed that such morphology of Ly α emission is indeed expected in their numerical simulation. It would be interesting to quantify the amount of massive stars and supernovae needed to produce such large shell-like structures.

Finally, do we see evidence of photo-ionization by intense starburst or AGN activity in LABs? The answer is ‘yes’, at least for many objects. Luminous sub-mm and mid-infrared emission are evidence of intense star formation and/or AGN activities. Geach et al. (2005) reported the sub-mm detection of in total of six LABs in SSA22 at $z = 3.1$ (but also see Matsuda et al. 2007 for SSA22-LAB1) and an LAB in the ‘Francis’ cluster (Francis et al. 2001). More than a few LABs, including the one at $z = 2.7$ discovered by Dey et al. (2004) and 8 LABs in SSA22 at $z = 3.1$, and three LABs in the Francis cluster (Francis et al. 2001) are associated with the Spitzer MIPS $24\mu\text{m}$ sources (Webb et al. 2008, submitted; Colbert, in this workshop). Significant PAH emission is observed for the majority of the LABs detected in MIPS $24\mu\text{m}$ (Colbert, this workshop).

Evidence of AGN activity is also seen in several LABs. Geach et al. (this workshop) showed that X-ray sources with luminosity $L_X = 10^{44-44.3} \text{ erg s}^{-1}$ were associated with four, or possibly five ($\sim 17\%$ of the observed) LABs at $z = 3.1$ in SSA22. Their luminosity is comparable to, or larger than, the Ly α luminosity and thus the Ly α emission may be powered by the photoionization of AGNs. They are all associated with the $8\mu\text{m}$ sources detected in the Spitzer IRAC images. Webb et al. (2008) also studied the $8\mu\text{m}$ sources associated with the LABs in SSA22. For the six $8\mu\text{m}$ sources, of which four are detected in X-ray in Geach et al., their NIR-MIR colors are located between sub-mm galaxies and luminous quasars. Many of them must host AGN and intense dusty star formation is likely to take place together. Weidinger et al. (2004; 2005) found significantly extended Ly α emission around a hidden AGN. In total, $\sim 20\%$ of LABs at $z = 3.1$ in SSA22 show evidence of AGN activity.

4 Physical Properties of LABs

We then discussed the physical properties of LABs, such as sizes, masses, kinematics, dust extinction, metallicity, and clustering. As the time was limited, we focused on their stellar masses and clustering properties.

Uchimoto et al. (2008) studied the stellar masses of the continuum sources which are found to be (by their spectroscopic redshift) or likely to be (by their photometric redshift) associated with the LABs in SSA22. They found that the total stellar masses of the sources associated with each luminous LABs spans $10^{10-11} M_{\odot}$ and are correlated with the $\text{Ly}\alpha$ luminosities. Webb et al. (2008) showed that a large fraction of LABs are detected in the IRAC 3.6 μm band, which indicate that their stellar masses are larger than $\sim \text{several} \times 10^9 M_{\odot}$. These stellar mass values are significantly larger than LAEs, whose stellar masses are typically $\sim 10^{8-9} M_{\odot}$. Thus, the results are consistent with that LABs with 30 – 100 kpc size, in contrast to the samples of typical LAEs, are associated with stellar massive galaxies at high redshift. A word of caution is that the results are so far limited to the LABs in SSA22 (Matsuda et al. 2004). In order to reveal the general properties, observations in other field are badly needed.

Matsuda et al. (in this workshop) presented the preliminary results of their extended SSA22 survey. They detected 89(9) LABs larger than 30 kpc (60 kpc) over a 1.4 deg^2 field including the original SSA22-Sb1 area (Matsuda et al. 2004) and found that they are highly clustered in the central ~ 30 Mpc region. The idea that LABs are massive objects seems to be consistent with that they are highly clustered. Many LABs are in the dense environment of star-forming galaxies (Keel et al. 1999; Steidel et al. 2000; Matsuda et al. 2004, also this workshop; Prescott et al. 2007). However, some of the LABs detected by Saito et al. are not in a dense environment (Saito, this workshop). As the LABs in Saito et al. (2006; 2008) were selected by a rather different manner (i.e., $2 \times$ half-light radius of 1.4-4 arcsec, and a spatially-extended spectrum rather than isophotal area), it is not clear if they are a similar population and direct comparison is difficult. It is true that we need more data to really conclude if giant LABs are only seen in dense environments.

5 So, What Are LABs?

So, what are LABs? Observational results obtained so far strongly suggest that the majority of 30 – 100 kpc LABs are massive galaxies (supported by the stellar mass and strong clustering of them). A significant fraction of AGN association is not inconsistent with the idea, as AGNs seems exclusively asso-

ciated with massive objects even at these redshift. Together with the evidence of large velocity width, sub-mm and MIR detection, many of these objects experience intense star-formation events and probably have super-wind activities (by large velocity width). Thus, we may tentatively conclude, or at least set a likely working hypothesis that the majority of 30 – 100 kpc LABs are massive young galaxies in their formation phase, although more detailed quantitative arguments are absolutely needed in the future.

On the other hand, the origin of extended Ly α emission, especially of giant LABs (50 – 150 kpc), seems still unclear and heterogeneous. There are candidates of cooling collapse objects, galactic super-wind objects, and evidence of AGN ionization. LABs are still mysterious objects, and in fact a mixture of these processes may explain their nature.

One very interesting result is the report by M. Prescott in this workshop of the detection of extended HeII emission in an LAB at $z = 1.7$. What is the origin(s) of the clearly extended HeII emission? The intensive study of LABs should be continued.

6 Final Remarks

I could not record all the invaluable comments and questions during the discussion and thus am afraid this report may not be a complete record of the discussion and just the description along the line presented. It was indeed a useful discussion to summarize the current understanding and consider the future prospects. Let me thank again for the workshop organizers and the participants to the discussion.

References

- Christensen, L., Jahnke, K., Wisotzki, L., & Sánchez, S.F., 2006, A&A, 459, 717
Dey, A., Bian, C., Soifer, B.T., et al., 2005, ApJ, 629, 654
Dijkstra, M., Haiman, Z., & Spaans, M., 2006, ApJ, 649, 37
Fardal, M.A., Katz, N., Gardner, J.P., et al., 2001, ApJ, 562, 605
Ferguson, H.C., Dickinson, M., Giavalisco, M., et al., 2004, ApJL, 600, L107
Francis, P.J., Williger, G.M., Collins, N.R., et al., 2001, ApJ, 554, 1001
Geach, J.E., Matsuda, Y., Smail, I., et al., 2005, MNRAS, 363, 1398
Geach, J.E., Smail, I., Ellis, R.S., et al., 2006, ApJ, 649, 661
Greve, T.R., Stern, D., Ivison, R. J., et al., 2007, MNRAS, 382, 48
Haiman, Z., Spaans, M., & Quataert, E., 2000, ApJL, 537, L5

- Keel, W. C., Cohen, S. H., Windhorst, R. A., & Waddington, I., 1999, *AJ*, 118, 2547
- Matsuda, Y., Yamada, T., Hayashino, T., et al., 2004, *AJ*, 128, 569
- Matsuda, Y., Yamada, T., Hayashino, T., Yamauchi, R., & Nakamura, Y., 2006, *ApJL*, 640, L123
- Matsuda, Y., Iono, D., Ohta, K., et al., 2007, *ApJ*, 667, 667
- Mori, M., & Umemura, M., 2006, *Nature*, 440, 644
- Nilsson, K.K., Fynbo, J.P.U., Møller, P., Sommer-Larsen, J., & Ledoux, C., 2006, *A&A*, 452, L23
- Ohyama, Y., Taniguchi, Y., Kawabata, K.S., et al. 2003, *ApJL*, 591, L9
- Ouchi, M., Ono, Y., Egami, E., et al. 2009, *ApJ* in press, arXiv:0807.4174
- Palunas, P., Teplitz, H.I., Francis, P.J., Williger, G.M., & Woodgate, B.E., 2004, *ApJ*, 602, 545
- Prescott, M.K.M., Kashikawa, N., Dey, A., & Matsuda, Y., 2008, *ApJL*, 678, L77
- Saito, T., Shimasaku, K., Okamura, S., et al., 2006, *ApJ*, 648, 54
- Saito, T., Shimasaku, K., Okamura, S., et al., 2008, *ApJ*, 675, 1076
- Smith, D.J.B., & Jarvis, M.J., 2007, *MNRAS*, 378, L49
- Steidel, C.C., Adelberger, K.L., Shapley, A.E., et al., 2000, *ApJ*, 532, 170
- Uchimoto, Y.K., Suzuki, R., Tokoku, C., et al., 2008, *PASJ*, 60, 683
- Weidinger, M., Møller, P., & Fynbo, J.P.U., 2004, *Nature*, 430, 999
- Weidinger, M., Møller, P., Fynbo, J.P.U., & Thomsen, B., 2005, *A&A*, 436, 825
- Wilman, R.J., Gerssen, J., Bower, R.G., et al., 2005, *Nature*, 436, 227
- Yang, Y., Zabludoff, A.I., Davé, R., et al., 2006, *ApJ*, 640, 539